Freie Universität Berlin

Dendritic Polyglycerol-Based Degradable Nanogels for Transport and Delivery of Bioactive Molecules

DISSERTATION

zur Erlangung des akademischen Grades des

Doktors der Naturwissenschaften (Dr. rer. nat.)

eingereicht im Fachbereich Biologie, Chemie, Pharmazie

der Freien Universität Berlin

vorgelegt von

Xuejiao Zhang

aus Liaoning, China

Berlin, April 2015

The results presented in this thesis were performed from September 2011 to April 2015 at the Institut für Chemie und Biochemie of the Freie Universität Berlin under the supervision of Prof. Dr. Rainer Haag.

1st Reviewer: Prof. Dr. Rainer Haag, Freie Universität Berlin

2nd Reviewer: Prof. Dr. Beate Koksch, Freie Universität Berlin

Location of Defense: 34.16/17, Takustr. 3, 14195 Berlin

Date of Defense: 24th June, 2015

Acknowledgements

First and foremost I would like to thank Prof. Dr. Rainer Haag for giving me this great opportunity to conduct my PhD research in his group. I appreciate that he always supports my research interests and gives me sufficient freedom to fulfill my own ideas. Meanwhile, he provides me plenty of scientific suggestions, which is a great help for accomplishing my projects and for my future carrier.

I also thank Prof. Dr. Beate Koksch for being the second referee and spending her valuable time to review my thesis.

Moreover, I thank Jr.-Prof. Dr. Marcelo Calderon and his group members for having me in their nanogel subgroup. I have gained much knowledge from their presentations and discussions.

I would like to acknowledge Dr. Katharina Achazi for introducing me the basic principles and operation techniques in the Biolab. She is a great help in conducting the biological experiments of all my projects and has contributed many precious suggestions as well. I appreciate Kai Zhang for helping me with the biological tests. I thank Dirk Steinhilber for teaching me the basic knowledge and the method of nanogel preparation.

Furthermore, I thank Dr. Stefanie Wedepohl, Christina Kühl, and all the other members in the Biolab for their patient explanations and great help during my experiments.

I would like to especially thank Dr. Pamela Winchester for the proofreading of the manuscripts. I would like to thank Jutta Hass, Dr. Wiebke Fischer, Christiana Halsdorfer, Achim Wiedekind, and Gaby Hertel for the great support in chemical ordering, lab techniques, as well as all the other issues.

I appreciate all the research facilities in the Institute of Chemistry and Biochemistry, and would like to particularly thank Dr. Andreas Schäfer, Dr. Andreas Springer, and their colleagues for their help with MS and NMR measurements. I thank Andrea Schulz and Dr. Christoph Böttcher for helping me with the TEM measurements.

I thank the China Scholarship Council (CSC) for providing me the financial support during my whole PhD period.

Finally, I am very thankful to my parents and friends for their care throughout all these years. Only with their support and encouragement, could I finish my studies in Germany. I especially thank my best friend, Shuang Zhang, and her family, who helped us during a most difficult time in my family. I will never forget your assistance and hope our friendship will last forever.

Table of Contents

1 Introduction

1.1 Drug delivery systems

Many therapeutic molecules (anticancer drugs, photo-sensitizers, and anti-oxidants) as well as biomacromolecules (proteins, peptides, and DNA/RNA) are not very efficacious because of their low solubility, instability, and cytotoxicity.[1] Ideally, therapeutics are essentially transferred to the targeted cells and then released in the cell organelles (e.g. cytoplasm or nucleus). Drug delivery systems (DDSs) have emerged as a promising approach for specifically delivering therapeutics to the site of action. Since Liposomal amphotericin B was firstly approved by FDA as a drug delivery system in 1990, more than 10 DDSs have become commercially available to treat diverse diseases, such as cancer, fungal infections, and muscular degeneration (Figure 1).[2]

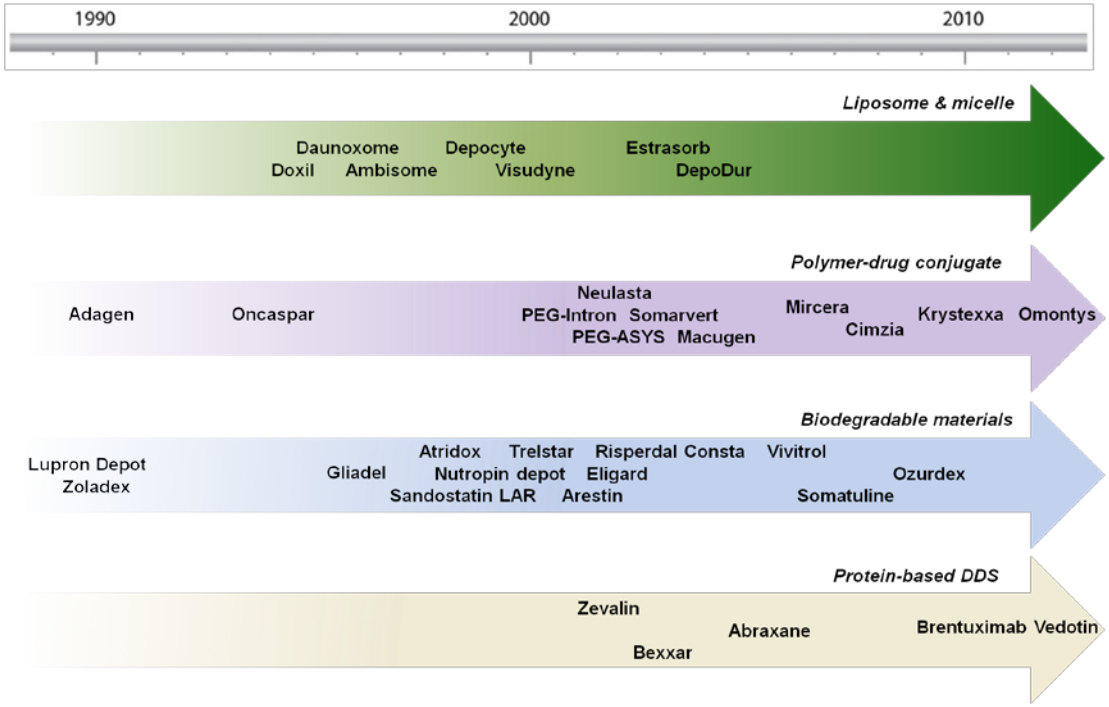

Figure 1. FDA approved DDS in the market. Reproduced from Ref. [2]. Copyright 2013 Elsevier Ltd.

Polymeric DDSs, including micelles,[3] liposomes,[4] nanoparticles,[5] nanogels,[6] and dendrimers[7] have been investigated as delivery vehicles for therapeutic molecules. They can increase the solubility of antitumor drugs, prolong circulation time, enhance the accumulation in the tumor tissue via the enhanced permeability and retention (EPR) effect, reduce the adverse effects, and improve the therapeutic efficacy.[8]

However, there are still some challenges for DDSs, such as stability during in vivo circulation, site-specific delivery, and controllable intracellular drug release.[1b, 9] Therefore, smart DDSs that are responsive to certain stimuli are of great interest. They offer a way to enhance cellular uptake, prevent premature drug release, release the drug in a precise and controllable manner, and increase the drug bioavailability.[1a]

1.1.1 Physical encapsulation

Depending on the preparation method, a drug can either be physically encapsulated in the polymeric carriers or covalently bound to the polymeric scaffold. The non-covalent method requires hydrophobic interactions, electrostatic interactions, or hydrogen bonds between the polymeric carriers and the entrapped drug molecules for drug encapsulation. Drugs can be introduced either in the process or after the formation of the respective carrier systems. Compared to covalent conjugation, this method is relatively simple to perform, because the polymers and drugs do not have to be chemically modified. Labile molecules can be protected by encapsulation in the nanocarriers, which improves the hydrophobic drugs' solubility. However, several obstacles for the encapsulation approach still exist. During in vivo circulation, a drug may prematurely release because of the low stability of nanocarriers. Moreover, the drug loading capacity varies from batch to batch, which restricts its clinical application. Furthermore, some carrier systems possess a low drug loading capacity that is inadequate for an efficient therapy.[10] Crosslinked DDSs, such as crosslinked micelles[11] or nanogels,[12] can provide a more stable encapsulation matrix compared

to non-crosslinked ones.

1.1.2 Covalent conjugation

In addition to physical encapsulation, covalent conjugation of therapeutic molecules to a polymeric carrier is another approach to improve bioavailability. Polymer-drug conjugation has been widely exploited to improve therapeutic properties of peptides,[13] proteins,[14] anticancer drugs,[15] and oligonucleotides.[16] Several prodrug systems have been in the different stages of clinical trials.[15b, 17]

Chemical conjugation allows better batch-to-batch consistency than physical encapsulation because it allows precise control of the drug loading percentage. In addition, polymer-drug conjugates normally possess prolonged circulation half-life, increased solubility of hydrophobic drugs, improved stability, suppressed premature drug release, and enhanced drug efficacy.[18] By introducing sensitive linkers, controlled drug release can be manipulated in response to biological stimuli, such as pH, temperature, and enzymes.[19] There are some potential limitations of this approach. For example, many therapeutic molecules do not possess functional groups for conjugation, which limits their universality. Additionally, conjugation of drugs to polymeric carriers may inactivate the drug.

1.1.3. Tumor targeting

1.1.3.1 Active targeting

Incorporating targeting ligands to recognize tumor specific receptors, so-called active targeting, has been extensively applied to improve tumor cellular uptake of nanocarriers.[8a] The ligands include large antibodies and small molecular ligands that have high specificity and affinity towards target cells with overexpressed receptors. They are able to improve the cellular uptake of carrier systems via receptor-mediated endocytosis.[20] Some actively targeting nanosystems, however, may have

non-specific bindings or immunogenicity that could induce decreased in vivo circulation time and lower tumor penetration. Moreover, active targeting can only trigger cellular uptake after accumulation into the tumor tissue, which still depends on the passive targeting via the EPR effect.[21]

1.1.3.2 Passive targeting

Passive targeting is based on the EPR effect. As shown in Figure 2, tumor blood vessels are normally more porous than blood vessels in normal tissue. Small molecules can diffuse into both normal and tumor tissue, whereas macromolecules can only enter tumor tissue with leaky endothelial capillaries. Moreover, the lymphatic drainage system in tumor tissue is generally defective so that the macromolecules tend to be retained and accumulated in solid tumors.[8d, 22] By controlling the size of the carrier systems, a higher local concentration of nanocarriers can be achieved in a tumor site than in normal tissue.[23] The passive targeting drug delivery systems are universal and easy to prepare compared to the active targeting approach, since the EPR effect is applicable for nearly all kinds of rapidly growing tumors.[24] To avoid kidney filtration and clearance by the liver and reticuloendothelial system (RES), nanocarriers in the range of 10 to 200 nm are suitable for EPR effect.[20, 25]

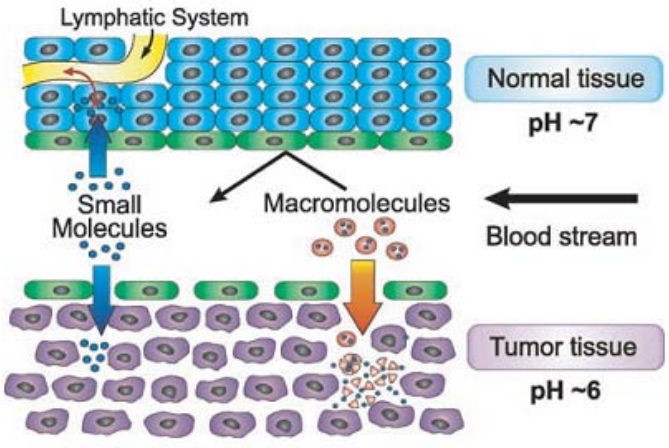

Figure 2. Schematic illustration of the enhanced permeability and retention (EPR)

effect. Reprinted with permission from Ref. [22]. Copyright 2006 Wiley-VCH.

1.2 Nanogel formation

Nanogels are nanosized hydrogel particles with three-dimensional networks composed of crosslinked polymer chains.[26] In recent years, they have obtained more attention because of their superior properties to other delivery systems, such as high water content, exceptional stability, biocompatibility, and adjustable chemical and mechanical properties, [19, 27] These unique properties provide great opportunities for the application of nanogels in the biomedical field, such as tissue engineering, sensing, diagnostics, and, most importantly, in drug delivery.

1.2.1 Covalent crosslinking

Nanogels formed by covalent crosslinking, including polymerization of low molecular weight monomers and crosslinking of macromolecular precursors, can maintain their stability under in vivo conditions. These nanogels can retain loaded drugs in the covalently crosslinked network better than supramolecularly crosslinked systems. However, crosslinking agents are usually employed in a traditional crosslinking reaction, which might induce undesirable cytotoxicity and destroy encapsulated fragile payloads like proteins, oligosaccharides, and cells.[26a, 28] Therefore, there has been more and more exploration of biocompatible reactions in the field of biomedical gelation.

1.2.1.1 Nanogel preparation from low molecular weight monomers

Radical polymerizations, especially living radical polymerizations, are normally applied in synthesizing nanogels from small molecular monomers.[29] This kind of polymerization is initiated by free radicals that are generated from the initiators, and

the nanogel network is formed by crosslinking monovinylic monomers with di- or multifunctional crosslinkers.[29a] The reaction occurs within the preformed heterogeneous colloidal droplets, normally via (inverse) miniemulsion.[19] Compared to traditional radical polymerization, living radical polymerization, normally atom transfer radical polymerization (ATRP), is advantageous for making nanogels with preferable properties, such as higher swelling ratios, better colloidal stability, more homogeneous structures, and controllable degradation.[30]

1.2.1.2 Crosslinking of macromolecular precursors

Di-functional or multi-functional macromolecules can be crosslinked to form nanogels via click chemistry, Schiff-base reaction, thiol-disulfide exchange reaction, photo-induced crosslinking, etc. (Table 1). Ideally, nanogels for biomedical applications should be formed under mild conditions, which are catalyst free, relatively low temperature, and bioorthogonal.

1.2.1.2.1 Bioorthogonal reactions

Bioorthogonal reactions are first defined by Carolyn R. Bertozzi as chemical reactions that can occur in living systems without interacting or interfering with the native biochemical processes. The functional groups should be able to selectively react with each other under conditions that are nontoxic to cells and organisms. Bertozzi et al . have developed two bioorthogonal transformations: the Staudinger Ligation and strain-promoted azide-alkyne cycloaddition (SPAAC) by exploiting azide as the promising functional group due to its special features, like small, abiotic, and bioinert. [31]

1.2.1.2.2 Click chemistry

Click chemistry, including copper-catalyzed azide-alkyne Huisgen cycloaddition (CuAAC) and copper-free click reactions, such as SPAAC, thiol-ene click reaction, and Michael addition, has been applied to crosslink macromolecular precursors with reactive functional groups to form nanogels.[26a]

CuAAC has been utilized to synthesize hydrophilic nanogels for bioimaging and therapeutic drug delivery.[8a, 32] In CuAAc reactions, both azides and alkynes are inactive to biomolecules, which is a prerequisite for the formation of biomaterials.[33] Moreover, the CuAAC reaction is normally performed under mild conditions without yielding any byproducts. However, the copper catalysts possess cytotoxicity towards living cells so that the incomplete removal of copper catalysts can hamper the in vivo applications.[34] Therefore, copper-free click reactions can be advantageous.

It is possible to fabricate nanogels without any toxic catalysts by copper-free click reactions, including SPAAC, thiol-ene click reaction, and Michael addition reaction, which are beneficial for the biomedical applications.[35]

SPAAC has been developed as an alternative to CuAAC for generating hydrogels for biomedical applications, especially for tissue engineering, due to its non-cytotoxicity and high efficiency.[36] Our group has fabricated pH-cleavable cell-laden microgels by bioorthogonal SPAAC for the encapsulation and programmed release of cells.[37]

In the thiol-ene reaction, thiols are reacted with unsaturated groups, such as alkenes, without the need of a metal catalyst. Hyaluronic acid (HA) nanogels have been fabricated using a thiol-ene reaction between pentenoate and thiol groups under UV irradiation.[38]

In addition to SPAAC and thiol-ene reactions, Michael addition reaction is another copper-free click reaction. It is the base-catalyzed nucleophilic addition of Michael donor to a Michael acceptor, normally an activated α,β-unsaturated carbonyl-containing compound.[39] Recently, Seiffert et al. have developed cell-laden microgels by nucleophilic Michael addition reaction via a microfluidic device.[40]

1.2.1.2.3 Schiff-base reaction

The Schiff-base reaction occurs between aldehydes or ketones and amines or hydrazide containing compounds with high reaction rates under mild conditions. The aromatic carbonyl is more favorable than the aliphatic carbonyl concerning the thermodynamic balance of the reaction.[41] In addition, compared to a ketone carbonyl, aldehyde carbonyl groups have a much higher reactivity. Therefore, benzaldehyde is a promising reactant in Schiff-base reaction.[42] The formed imine bond is labile at acidic pH and can potentially serve as pH-responsive linkers. The Schiff-base reaction has been used to synthesize nanogels by crosslinking alginic aldehyde and gelatin in the presence of borax.[43]

1.2.1.2.4 Thiol-disulfide exchange reaction

The thiol-disulfide exchange reaction is a fundamental process in biological systems for the formation of a cellular disulfide bond.[44] In the reaction, a free thiol is deprotonated to form a reacting species, thiolate anion ($-S^-$), which displaces one sulfur of the disulfide bond in the oxidized species through an S_N2 transition state.[45] This reaction is widely used in synthesizing nanogels.[26b, 46] Thayumanava et al. have fabricated a series of nanogel systems based on the thiol-disulfide exchange reaction, which causes a self-crosslinking of pyridyl disulfide containing amphiphilic polymers.[47]

1.2.1.2.5 Other crosslinking reactions

There are some other reactions, including photoreaction, amide-based reaction, boronic acid-diol complexation, and enzyme-catalyzed reaction, have been used for the formation of nanogel.

Table 1. Covalent crosslinking reactions for nanogel formation.[26a]

Reactions		*Reacting groups*	*Reaction conditions*
Radical polymerization		Free radical	Heating, light, or redox initiated
CuAAC		Azide and alkyne	Copper catalyzed
Copper free click chemistry	SPAAC	Azide and cyclooctyne	pH 7.4
	Thiol-ene	Thiol and unsaturated groups (alkenes)	Radical initiated (photo-irradiation)
	Michael addition	Thiol and α, β-unsaturated carbonyl group (acrylates and maleimides)	pH 6-8, no catalyst
Schiff-base reaction		Aldehyde and amine or hydrazide	no catalyst
Thiol-disulfide exchange reaction		Thiol and disulfide	pH > 8
Photo-induced crosslinking		Coumarin or alkene	UV irradiation, photo initiator
Amide-based crosslinking		Amine and carboxylic acids or activated ester	No additive needed
Boronic-diol complexation		Boronic acid and diols	pH > pK_a of boronic acid
Enzyme-catalyzed crosslinking		Thiol	HRP catalyzed

Reactants containing a photo-activatable group can be crosslinked by photo irradiation.[48] Although photoreactions are highly efficient, the initiator may induce cytotoxicity in the produced gels.[49] Therefore, it is important to choose biocompatible photoinitiators to make gel networks.

Due to the high reactivity with carboxylic acids, activated esters, isocyanates, amine groups can be used for synthesizing nanogels.[19, 50] This facile methodology provides an opportunity to introduce various stimuli-response properties into the nanogels by modulating the structure of the diamine crosslinker.[51]

The complexation between a boronic acid and 1,2- or 1,3-diols has been applied to fabricate hydrogels[52] and core-crosslinked micelles[53]. Recently, boronate esters have also been utilized to prepare nanogels.[54]

Enzyme-catalyzed crosslinking has been used for the preparation of hydrogels as an innovative technology with greater efficiency than other crosslinking methods due to its short reaction time, mild reaction condition, and high biocompatibility.[55] The gelation kinetics, depending on the structure and composition of the macromer, the ratio of the reactants, and the enzyme concentration, are well-controllable. Therefore, enzyme-catalyzed reactions are suitable for in situ gelation systems. Our group developed biocompatible nanogels based on dendritic polyglycerol by horseradish peroxidase (HRP) catalyzed crosslinking for protein encapsulation.[56]

1.2.2 Supramolecular crosslinking

Supramolecularly crosslinked nanogels involve self-assembled aggregations based on non-covalent interactions including ionic,[57] Van der Waals',[58] and hydrogen bonding[59] between polymer chains. The supramolecular crosslinking is conducted under mild conditions without producing any byproducts or requiring any crosslinking agent and catalyst that may cause toxic effects. Therefore, it is favorable for biomedical applications.[26a] However, it is difficult to prepare nanogels via

supramolecular crosslinking with high stability and controllable size since the non-covalent interaction is not strong enough.[26c] Hence, their reduced stability makes them less applicable under the harsh in vivo systems than covalently crosslinked nanogels.[60] To improve their mechanical properties, multivalent systems containing multiple interactions can be applied.[61]

1.3 Preparation methods for nanogels

1.3.1 Precipitation polymerization

Precipitation polymerization is commonly used to synthesize thermoresponsive nanogels.[62] The monomer (N-isopropylacrylamide, NIPAm) and a crosslinking agent (N,N'-methylenebis(acrylanide), BIS) are dissolved in water to form a homogeneous mixture that is heated to the temperature above the LCST of pNIPAm. Ammonium or potassium persulfate (APS/KPS), which decomposes at the reaction temperature, is added to initiate the polymerization. The elevated reaction temperature favors the homogeneous nucleation process, in which the growing polymer chains collapse to form particles.[63]

1.3.2 Inverse miniemulsion polymerization

Inverse miniemulsion polymerization is a water-in-oil (W/O) polymerization process that forms kinetically stable aqueous droplets containing water-soluble monomers. With the aid of oil-soluble surfactants, stable dispersions are formed at, below, or around the critical micellar concentration (CMC) in a continuous organic medium by sonification. The hydrogel particles are produced in the polymerization process within the aqueous droplets.[30a, 63b] Biocompatible nanogels based on poly(ethylene oxide) were synthesized by ATRP in the process of inverse miniemulsion for the encapsulation of different bioactive molecules.[29d]

1.3.3 Microfluidic microgel formation

Microfluidics is a versatile technique to fabricate micrometer-sized hydrogel particles. In microfluidics, emulsion droplets are used as templates with controlled size, shape, and monodispersity for the formation of gel particles. In this approach, glass capillary devices or devices made by soft lithography, normally composed of polydimethylsiloxane (PDMS), can be used for droplet fabrication.[26a] In a flow focusing microfluidic device, monomers, crosslinkers, and initiators are added to the dispersed phase and form a laminar coflowing stream in a microchannel. Monodispersed, micrometer-sized premicrogel droplets are formed by the break-up of the stream, which is induced by flow focusing with immiscible paraffin oil (continuous phase) at the second cross-junction.[40] Microfluidics is an ideal approach to generate cell-laden microgels.[40, 64] Our groups has prepared pH-cleavable microgels by SPAAC reaction via droplet-based microfluidics for encapsulating and programmed releasing live cells.[37]

1.3.4 Particle replication in non-wetting templates (PRINT)

Particle replication in the non-wetting template (PRINT) method is a versatile method for fabricating monodispersed nanogels with various shapes.[28, 65] This micro-molding technique was first developed by the group of DeSimone in 2005.[66] A photocurable, perfluoropolyether (PFPE)-based elastomer (Fluorocur^{TM}) was prepared by soft lithographic techniques as a master template, which exhibits non-wetting behavior and possesses superior compatibility to most liquid materials. A liquid fluoropolymer is poured on the surface of the master template, photochemically crosslinked, and then peeled away. In this way, precise molds with micro- or nano-scale cavities are generated, which can be filled with macromonomer solutions. After the macromonomers are crosslinked, usually triggered by UV irradiation, the array of particles can be removed from the mold by using a harvesting film. Finally, the free flowing particles can be separated from the harvesting film.[67] This technique

enables the precise control over particle size from 20 nm to 100 μm with a large scale production potential.[68] Moreover, therapeutic cargos can be loaded with this method.[69] However, since the crosslinking reactions in soft lithography techniques require externally triggered initiation, which sometimes involves toxic radicals, their application for encapsulating fragile biomolecules is limited.

1.3.5 Inverse nanoprecipitation

The nanoprecipitation technique is a facile, mild, and low energy consuming process that has been applied for synthesizing hard and non-polar nanoparticles (e.g. PLGA)[70] or core-shell nanoparticles from amphiphilic block copolymers.[71] This technique is based on interfacial deposition because of the displacement of the solvent with the non-solvent.[72] The miscibility of the solvent and non-solvent is a prerequisite for nanoprecipitation. The technique starts with macromolecules aggregating to form nuclei that further aggregate and generate nanoparticles up to the colloidal stability point.

Our group first reported the application of the inverse nanoprecipitation technique for fabricating hydrophilic nanogels based on dendritic polyglycerol (dPG).[32a] After injecting the aqueous solution of polymeric precursor into the non-solvent acetone, the aqueous phase quickly diffuses into the acetone phase, which induces the collapse of dPG to aggregate. Meanwhile, the crosslinking progresses and induces the formation of a nanogel network (Figure 3). By adjusting the ratio of water to acetone or the concentration of precursors, nanogels with tunable size and low polydispersity are obtained.[26b]

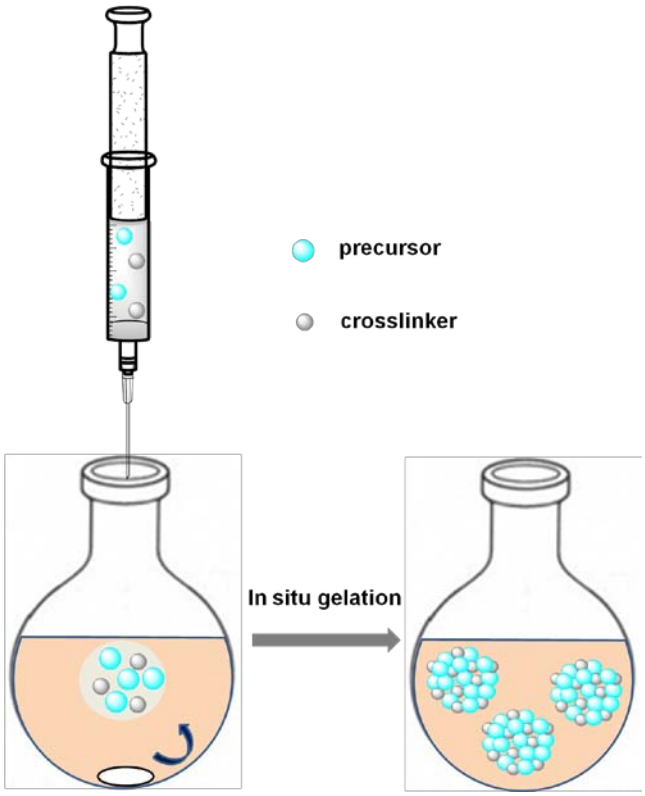

Figure 3. Nanogel formation by inverse nanoprecipitation.

1.4 Degradable nanogels

High stability is a prerequisite for drug delivery systems during blood circulation. Once reaching the site of action, the nanocarriers should be capable of releasing the entrapped therapeutic drugs to exert the biological functions. Degradable nanogels crosslinked with reversible linkages have been used to realize these goals. The dissociation of nanogels can be triggered by internal (pH, redox potential, and enzyme) or external (light and additives) stimuli at the target site, facilitating the drug release. Moreover, the body tends to eliminate the degraded nanocarriers, which reduces the inherent toxicity of the carrier vehicles due to accumulation.[26a]

Table 2. Labile crosslinkers used in biodegradable nanogels.[26a]

Crosslinkers	Structure	Cleavable conditions
Hydrazone linker		pH 5.5, 100 % degradation within 200 min, 10 times faster than pH 7.5
Imine linker		pH 5, cleavable within 3 h
Acetal linker		bisacrylamide acetal with a p-methoxy substituent, pH 5, half-life 5.5 min; slightly acidic pH, complete hydrolysis < 1 h
Ketal linker		pH 5.5, half-life 2 h
Carboxylate ester		hydrolysis under physiological conditions
Boronate ester		pH 5, cleavage in 120 min
Ortho-nitrobenzyl ester		UV 315-390 nm
Biscoumarin		UV < 260 nm
Disulfide		DTT, TCEP, GSH
Phosphoester		phosphatase, phospholipase
Boronate ester		glucose/ATP

1.4.1 pH-induced degradation

The environment of tumor or inflammatory tissues (pH 6.5-7.0) is more acidic than normal tissue and blood (pH 7.4). During cellular uptake, the vehicles reach the cell organelles, endosomes (5.5-6.5) and lysosomes (4.5-5.5), with even lower pH values.[1b, 26a, 73] These pH gradients which exist in biological systems can be used to trigger the dissociation of acid-sensitive nanogel systems. Various acid-cleavable linkers, such as acetals,[32a, 74], ketals,[75] esters,[54b, 54c, 76], imine,[77] hydrazone,[78] and vinyl ether,[79] have been introduced into the nanogel network.

Recently, our group developed biodegradable dPG nanogels crosslinked with acid-labile benzacetal linkers via the inverse nanoprecipitation technique for protein encapsulation.[32a] By introducing substituent moieties into the para position of benzacetals, the acid cleavability could be manipulated, which facilitated the controllable hydrolysis kinetics at the desired pH.[37, 80]

Berkland's group generated poly(N-vinylformamide) (PNVF) nanogels with a pH-sensitive ketal-containing crosslinker for lysozyme encapsulation. The ratio of monomer to crosslinker and the pH conditions exerted significant impact on the half-life of nanogels.[75a]

Narain et al. have synthesized multi-responsive hydrogels and nanogels crosslinked with boronate ester, which could be cleaved under weakly acidic conditions or in the presence of excess glucose.[54b]

The group of Yang has prepared crosslinked gel particles with a benzoic-imine bond based on the Schiff-base reaction between amino and benzaldehyde groups. The crosslinked structures were stable under physiological conditions but dissociated at acidic pH due to the cleavage of imine linkages.[77, 81]

The acid-cleavable hydrazone bond, which is stable at neutral conditions and hydrolyzed at acidic pH, has been widely applied in biomedical materials.[82] Ma et al. has fabricated polypeptide nanogels with hydrazone crosslinkages formed from hydrazine and aldehyde. The pH-sensitive drug release was achieved due to the lability of hydrazone linkers.[78]

1.4.2 Reductive degradation

The redox gradients between the oxidizing extracellular medium and the reductive intracellular environments have been used to cleave the nanogels containing disulfide bonds.[8a, 26b, 29c, 46b, 83] The tripeptide glutathione (GSH) is the most abundant reducing agent in the intracellular environment. It exists in the millimolar concentration range (~1-11 mM) in the cytosol, which is up to 1000 fold higher than that in the extracellular fluids (~10 μM).[84] Moreover, it has been found that the GSH level is more elevated in cancer cells than in normal cells.[85] The disulfide bonds are stable in the blood stream but are efficiently cleavable under intracellular reductive conditions, which facilitates the rapid release of anti-cancer drugs at the target sites in cancer therapeutics.[85b, 86]

We recently designed redox-sensitive polyvinyl alcohol (PVA) nanogels with charge-conversional properties to improve the cellular uptake for enhanced anti-cancer efficacy.[8a] After internalization, the release of doxorubicin (DOX) was triggered by the increased GSH level in the cytosol.

1.4.3 Enzymatic degradation

Local drug release can be triggered by the enzymes since their concentration varies within different cells and tissues.[48c, 87] In enzymatically degradable gel systems, the mesh size is crucial for the access of enzymes to the cleavable sites, which is a decisive process for enzymatic degradation. Wang et al. fabricated polyphosphoester-containing enzymatically degradable nanogels by photo-crosslinking. The release of doxorubicin (DOX) was accelerated by the enzyme phosphodiesterase I catalyzing the degradation of phosphoester linker.[48c]

1.4.4 Photo-induced degradation

The cleavage of photolabile groups is easy to spatiotemporally control by delivering

the irradiation to the systems.[87b, 88] However, ultraviolet light in the range of mid UV (280-315 nm) and far UV (200-280 nm) could be problematic for biomedical applications. Moreover, photodegradation may generate cytotoxic free radicals,[89] which denature proteins and influence cellular behavior.[90] Therefore, it is essential to choose a feasible irradiation condition to perform the photodegradation reaction.

The ortho-nitrobenzyl group has been explored to fabricate photolabile materials for biomedical applications because it is biocompatibile and inert towards the fragile residues both before and after photodegradation.[91] A ortho-nitrobenzyl group containing photodegradable crosslinker has been used to prepare dual-responsive protein-loaded microgels, which exhibited an on-demand protein release due to the fast degradation induced by photo irradiation.

Additionally, coumarin can be photodimerized under UV irradiation ($\lambda > 310$ nm) to form crosslinked nanogels, which showed photocleavage under $\lambda < 260$ nm.[48a] However, these nanogels' biomedical application is limited due to the problematic irradiation wavelength.

1.4.5 Other degradable nanogels

Apart from the above-mentioned cleavable nanogels, the crosslinked network can also be dissociated by adding additives, such as glucose and ATP.[54b, 54c] Moreover, the reversible click reactions, inducing Retro-Diels-Alder reactions[92] and Retro-Michael addition reactions,[93] have been used to degrade hydrogels. However, the biomedical applications of these reactions are limited because they need harsh degradation conditions (high temperature,[94] ultrasonic,[95] organic solvents[92a]). Furthermore, the dissociation of supramolecular crosslinked nanogels can be triggered by external stimuli, such as UV irradiation[96] or additive addition.[57b, 97] [i]

[i] Parts of this introduction were previously published in a recent review (Ref. 26a: X. Zhang, S. Malhotra, M. Molina, R. Haag, *Chem. Soc. Rev.* **2015**, *44*, 1948-1973) which is quoted in the text, respectively.

2 Scientific goals

For efficient drug delivery, nanocarriers need to be stable during blood circulation for better cellular uptake efficiency and a more controllable drug release at the target sites.

Compared to other carriers, like micelles, liposomes, and polymeric prodrugs, nanogels have some superior features: high water content, biocompatibility, tunable size, large surface area for multivalent bioconjugation, and an interior network for the incorporation of biomacromolecules. The crosslinked structure of nanogels can retain its properties during in vivo circulation, which is a promising solution for the stability of nanocarriers.

Dendritic polyglycerol (dPG) possess a high biocompatibility, water solubility, and multi-functionality, which makes it a promising candidate for biomedical applications. Therefore, dPG is selected as the macromolecular precursor for the formation of nanogels within this thesis.

Inverse nanoprecipitation, which is a facile, surfactant free, and low energy consuming technique, is applied to fabricate the nanogels. Compared to other methods, it is more convenient. The size of nanogels is easily manipulated by changing the ratio of solvent to non-solvent and by adjusting the concentration of the precursors.

The surface charge exerts great impact on the biocompatibility of nanocarriers and their internalization ability as well and needs to be carefully investigated. The pH in tumor tissues is slight acidic, whereas it is neutral in normal tissues or blood stream. The pH-induced charge conversional carrier systems are negative during blood circulation but become positive once they reach the slightly acidic tumor tissues.

Intelligent nanocarriers that release the drug in response to environmental stimuli have been developed for improved therapeutic efficacy. The internal stimuli, including pH, redox potential, and enzymes, are most applicable, since they are intrinsic properties of cells and there is no toxic effect that could be induced by external stimuli. The stimuli-responsive vehicles can facilitate the drug release at

desirable locations inside the cells.

Disulfide bonds are stable under extracellular conditions, but are cleavable in the intracellular reductive environment. Nanogels crosslinked with disulfide bonds can be stable and retain the entrapped drugs under physiological conditions. Once they are internalized (Figure 4), the crosslinked structure dissociates under the reductive conditions in the cytosol, which facilitates the release of therapeutic molecules.

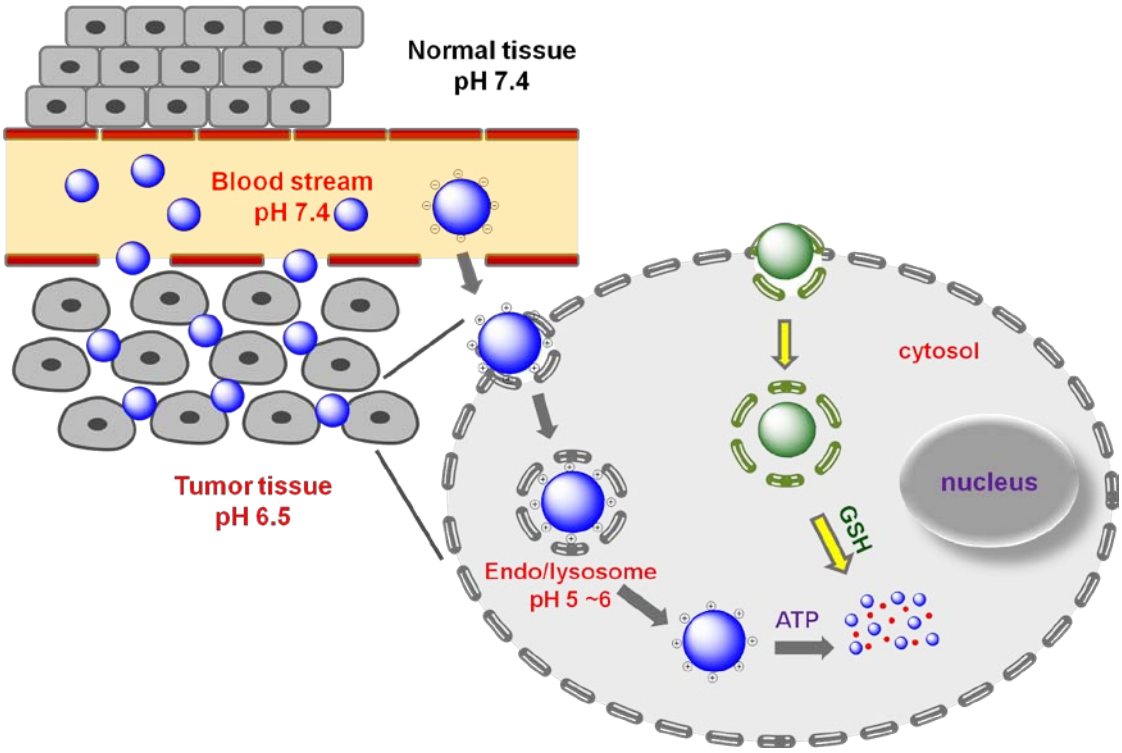

Figure 4. Pathway of biodegradable nanogels for intracellular drug delivery. The nanogels accumulate in the tumor tissue via the EPR effect. The negative surface charge is converted to positive from blood stream (pH 7.4) to tumor tissue (pH 6.5) due to the charge conversional property of nanogels. After internalization, the crosslinked structure dissociates in response to the internal signals (elevated concentration of GSH and ATP), which facilitates the intracellular drug release.

Boronic acids can form reversible boronate esters with the 1,2-diols in dPG. Introducing an aminomethyl to the ortho-position of the boronic acid can create a dative boron-nitrogen (B-N) interaction that can enhance the stability of boronate

esters at neutral pH. The boronate ester is labile at acidic pH and in the presence of a competing diol, such as adenosine-5’-triphosphate (ATP). The intracellular concentration of ATP is much higher compared to its extracellular concentration, which can stimulate the liberation of bioactive payload due to the nanogel dissociation (Figure 4).

This thesis will take advantage of cellular stimuli, including pH, redox potential, and ATP concentration gradients, to design new biodegradable nanogel systems for stimuli-responsive drug delivery.

3 Publications

3.1 Surfactant free preparation of biodegradable dendritic polyglycerol nanogels by inverse nanoprecipitation for encapsulation and release of pharmaceutical biomacromolecules

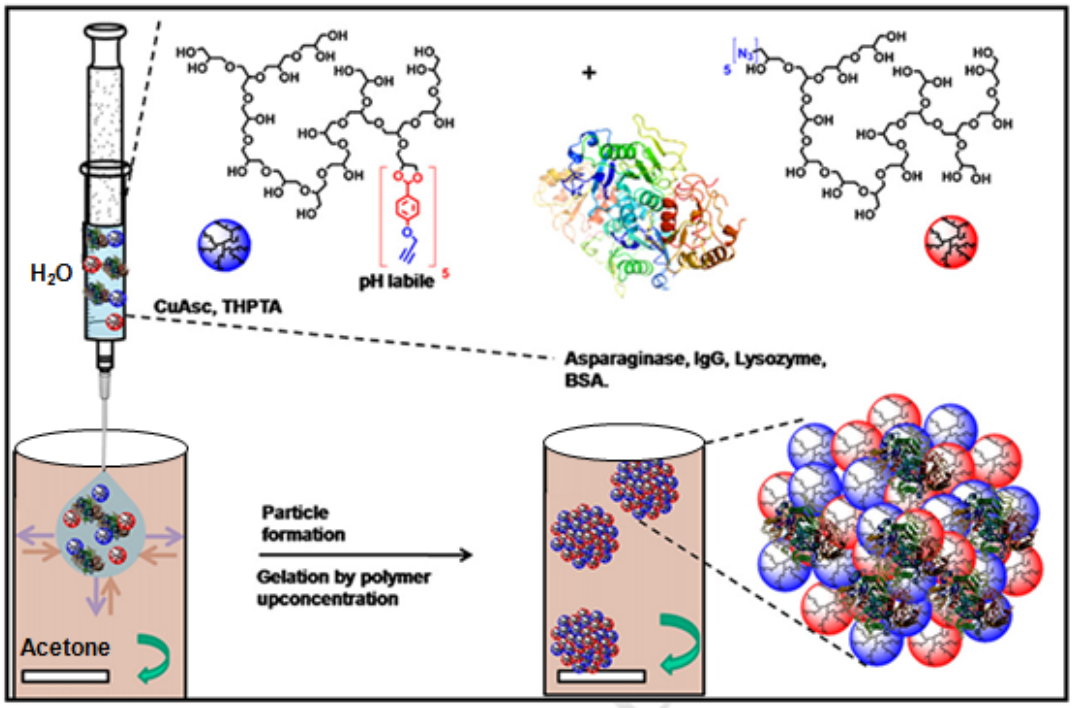

Dirk Steinhilber, Madeleine Witting, **Xuejiao Zhang**, Michael Staegemann, Florian Paulus, Wolfgang Friess, Sarah Küchler, Rainer Haag

J. Control. Release **2013**, *169*, 289-295.

http://dx.doi.org/10.1016/j.jconrel.2012.12.008

http://www.sciencedirect.com/science/article/pii/S016836591200836X

Author contributions

Dirk Steinhilber designed the project, performed the main experiments, and prepared the manuscript.

Madeleine Witting performed the enzyme release and activity and corrected the manuscript.

Xuejiao Zhang synthesized the macromolecular precursor and performed the preliminary protein loading experiments.

Michael Staegemann and Florian Paulus synthesized the macromonomer.

Wolfgang Friess and Sarah Küchler selected the enzyme and corrected the manuscript.

Rainer Haag corrected the manuscript and provided scientific discussions of the data.

3.2 A facile approach for dual-responsive prodrug nanogels based on dendritic polyglycerols with minimal leaching

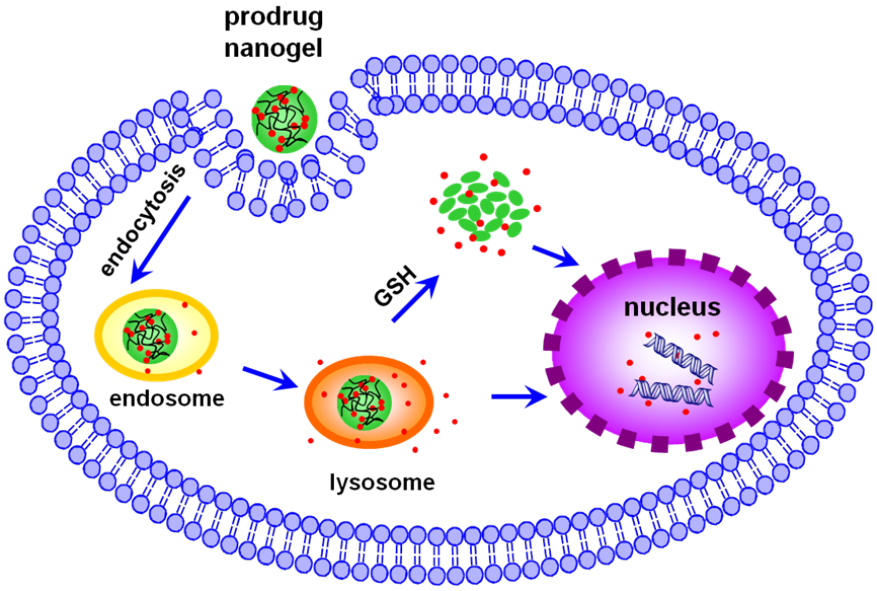

Xuejiao Zhang, Katharina Achazi, Dirk Steinhilber, Felix Kratz, Jens Dernedde, Rainer Haag

J. Control. Release **2014**, *174*, 209-216

http://dx.doi.org/10.1016/j.jconrel.2013.11.005

http://www.sciencedirect.com/science/article/pii/S0168365913008948

Author contributions

Xuejiao Zhang designed the project, performed the main experiments, and prepared the manuscript.

Katharina Achazi helped with the cellular experiments.

Dirk Steinhilber supervised the synthesis of nanogels via inverse nanoprecipitation.

Felix Kratz provided the DOX-EMCH.

Jens Dernedde supported the biological studies.

Rainer Haag supervised the project, provided scientific guidelines and suggestions, and revised the manuscript.

3.3 Boronate cross-linked ATP- and pH-responsive nanogels for intracellular delivery of anticancer drugs

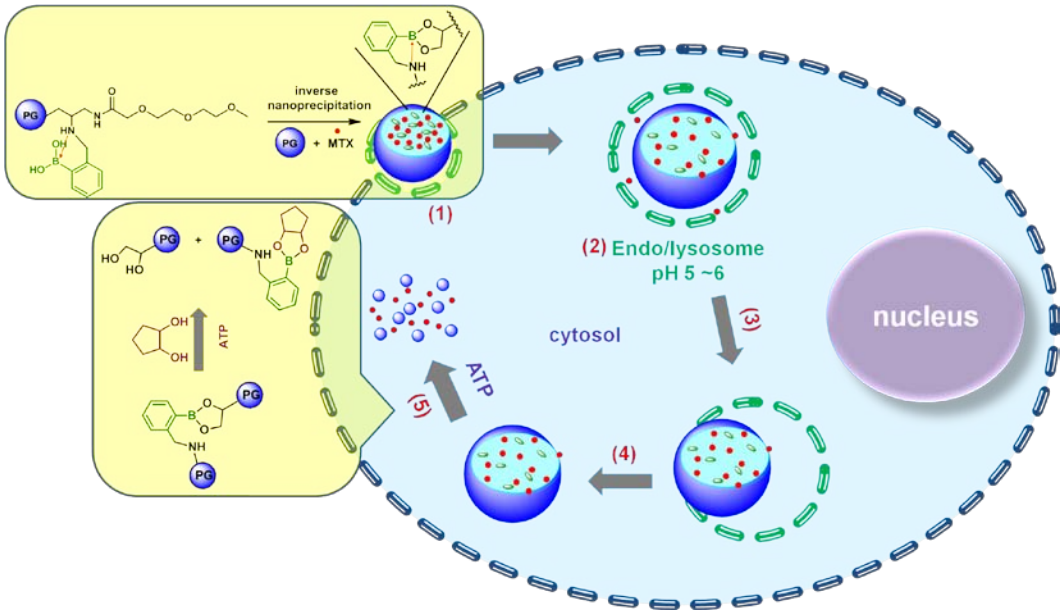

Xuejiao Zhang*, Katharina Achazi, Rainer Haag

Adv. Healthc. Mater. **2015**, *4*, 585-592.

http://dx.doi.org/10.1002/adhm.201400550

http://onlinelibrary.wiley.com/doi/10.1002/adhm.201400550/abstract;jsessionid=2610964BF3D0BB86FA09360313D701DC.f02t03

Author contributions

Xuejiao Zhang designed the project, performed the main experiments, and wrote the manuscript.

Katharina Achazi helped with the biological experiments.

Rainer Haag supervised the project, provided scientific guidelines and suggestions, and corrected the manuscript.

3.4 Multi-stage, charge conversional, stimuli-responsive nanogels for therapeutic protein delivery

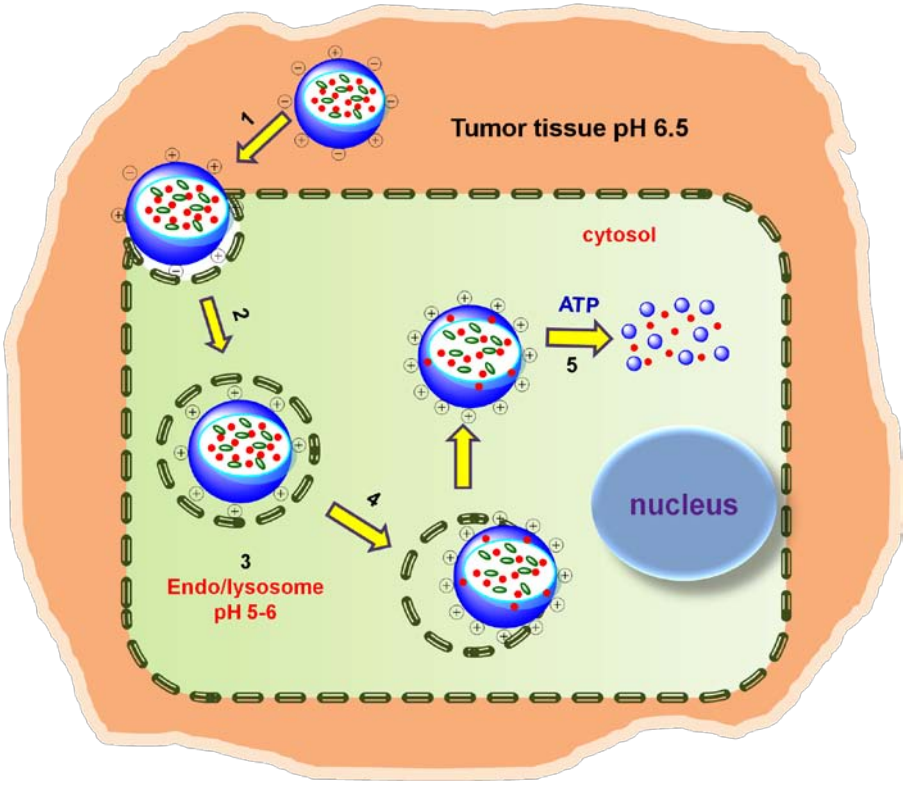

Xuejiao Zhang*, Kai Zhang, Rainer Haag

Biomater. Sci., **2015**, *accepted.*

Author contributions

Xuejiao Zhang designed the project, performed the main experiments, and wrote the manuscript.

Kai Zhang performed the cell apoptosis measurements and modified the manuscript.

Rainer Haag supervised the project, provided scientific guidelines and suggestions, and corrected the manuscript.

Multi-stage, charge conversional, stimuli-responsive nanogels for therapeutic protein delivery

Xuejiao Zhang[1,*], Kai Zhang[2], Rainer Haag[1]

1 Freie Universität Berlin, Institut für Chemie und Biochemie, Takustraße 3, 14195 Berlin, Germany

2 Charité-Universitätsmedizin Berlin, Institut für Laboratoriumsmedizin, Klinische Chemie und Pathobiochemie, 13353 Berlin, Germany

Corresponding author:
Xuejiao Zhang
Institute for Chemistry and Biochemistry
Freie Universität Berlin
Takustrasse 3, Berlin 14195 (Germany)
E-mail: zhangxuejiao1985@gmail.com

ABSTRACT

A boronate ester crosslinked zwitterionic nanogel (NGCA) with ATP/pH-sensitivity has been developed with an inverse nanoprecipitation technique to achieve a two-stage charge conversion that responds to tumor extracellular conditions (pH 6.5-6.8) and an intracellular acidic environment (pH 5-6). Cationic cytochrome C (CC), a therapeutic protein, has been encapsulated into NGCA through inverse nanoprecipitation via electrostatic interaction, to form protein-loaded nanogel (NGCA-CC). By adjusting the ratio of the amino and carboxyl groups in the nanogels, negatively charged nanogels that are safer under physiological conditions (pH 7.4) can convert their surface charge to positive at tumor extracellular pH, which enhance their cellular uptake efficiency. The citraconic amide formed from citraconic anhydride and amine can be cleaved in the intracellular acidic organelles to expose more amino groups and facilitate endosomal escape. The release of CC is accelerated in the presence of 5 mM ATP or under acidic conditions. Confocal laser scanning microscopy (CLSM) and flow cytometry have shown that NGCA-CC's cell uptake is higher at pH 6.5 than 7.4. MTT and real-time cell analysis (RTCA) have illustrated that there is more toxicity at pH 6.5 than at pH 7.4. The apoptosis process induced by CC was determined by flow cytometry.

Keywords: polyglycerol nanogel, charge conversion, protein delivery, nanogel degradation, cellular uptake

1. Introduction

Since the first FDA approved recombinant protein therapeutic human insulin entered the market in 1982, protein therapeutics have played a vital role for the treatment of various diseases, because of their high specificity, limited side effects, and predominant anticancer efficacy.[1-3] Various carrier systems have been developed to surmount the obstacles of protein therapeutics, such as instability, poor bioavailability, and low cell internalization efficiency.[4-6]

The surface charge exerts a great impact on the safety and stability of nanocarriers during blood circulation. Positively charged nanoparticles possess higher affinity with the negatively charged cell membrane, which facilitates cellular uptake, whereas their severe cytotoxicity, strong interactions with blood components, and rapid clearance often impede the in vivo applications.[7-9] Development of pH-induced charge conversional drug delivery systems can help to overcome the intrinsic pH difference between tumor tissues (pH 6.5-6.8) and normal tissues or blood stream (pH 7.2-7.4).[10-12]

Reactions of 2,3-dimethylmaleic anhydride (DMMA) and amino groups on the particle surface have been used to shield the positive charge of nanoparticles.[13-15] The generated amide bond is cleavable under mildly acidic conditions but stable at neutral or basic pH,[16] whereas the DMMA-decorated nanoparticles are inert under physiological conditions. After accumulating in the acidic tumor tissue through the enhanced permeation and retention (EPR) effect, the amide bond slowly cleaves and thus exposes the positive charge which eventually promotes cell internalization.[17] However, the cleavage of the amide bond is not prompt so that the charge conversion is delayed. Furthermore, the amide bond can also be slowly cleaved at neutral pH, but this is not propitious for long-term in vivo circulation.[18]

Zwitterionic nanoparticles with both anionic and cationic surface moieties, on the other hand, can rapidly change their surface charge at their isoelectric pH.[19,20] By adjusting the ratio of anionic and cationic components, instantaneous charge conversion from negative to positive can be achieved under tumor extracellular pH, which enhances internalization efficiency.

Another challenge for protein delivery is the acidic environment of cellular organelles. After endocytosis, the pH drops to 5-6 in the endosome/lysosome, where both the nanoparticles and their protein payloads can be degraded by endolysosomal acid and hydrolyase.[19] Therefore, it is necessary for the nanocarriers to liberate their encapsulated proteins into the cytoplasm through endosomal escape. Kataoka et al. have reported that citraconic amide, formed from citraconic anhydride and primary amines, cleaved at endosomal pH and induced the release of primary amines that promoted the endosomal escape of the protein into cytoplasm by disrupting the endosomal membrane.[11,21,22]

We here present a zwitterionic nanogel with two-stage charge conversional properties that we designed to respond to slightly acidic tumor extracellular conditions (pH 6.5-6.8) and an intracellular acidic environment (pH 5-6). As shown in Figure 1, the negatively charged zwitterionic nanogels become positive once accumulating into slightly acidic tumor tissue, which favors their endocytosis. Hydrolysis of citraconic

amide in the acidic intracellular organelles (endo/lysosome) exposes more amine groups and results in the second-stage charge conversion. The more elevated positive charge presumably interrupts the endo/lysosome membrane and facilitates endosomal escape. The high concentration of ATP made the nanogels degrade in the cytosol, which induced the protein release.

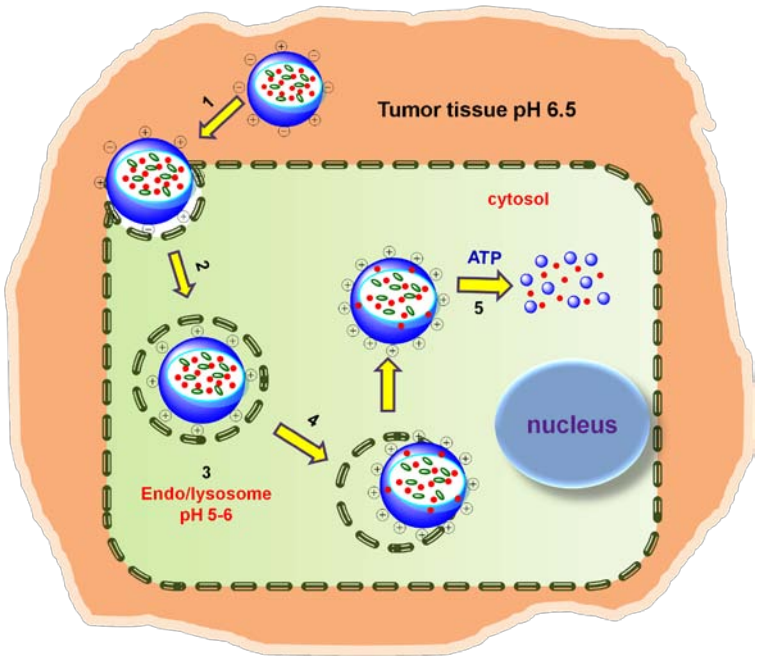

Figure 1. Schematic illustration of a two-stage charge conversion process of zwitterionic nanogels. (1) First stage charge conversion: from negative to positive owing to the decreased pH in tumor tissue compared to blood circulation, (2) cellular uptake by endocytosis, (3) second stage charge conversion: elevated positive charge due to the hydrolysis of citraconic amide, (4) endosomal escape, (5) dissociation of nanogels and drug release triggered by ATP in the cytosol.

2. Materials and Methods

2.1. Materials

dPG (M_n = 5.8 kDa, M_w = 7.5 kDa, PDI = 1.29) was synthesized based on the published procedure.[23,24] 2-formylphenylboronic acid (FPBA), fluorescein isothiocyanate (FITC), and cytochrome C (CC) were purchased from Sigma-Aldrich (Germany). 4'6-diamidino-2-phenylindole (DAPI), FM® 4-64 Dye (*N*-(3-Triethylammoniumpropyl)-4-(6-(4-(diethylamino) phenyl) hexatrienyl) pyridinium dibromide), and Dead Cell Apoptosis Kit with Annexin V Alexa Fluor® 488 & propidium iodide (PI) were purchased from Lifetechnology (Germany). All other chemicals were purchased from Aldrich (Germany) or Acros (Germany). For cell culture experiments, MCF-7 cells (DSMZ no.: ACC 115) cultured in RPMI supplemented with 10% fetal calf serum, MEM nonessential amino acids, 1 mM sodium pyruvate, and 10 µg/ml human insulin in a humidified atmosphere (5% CO_2) were used.

2.2. Characterization

^{1}H NMR spectra were recorded on a Bruker ECX 400. The residual deuterated solvent peaks were used as internal standard to calibrate the chemical shifts. The size and zeta potential were determined by a Zetasizer Nano-ZS from Malvern Instruments equipped with a 633 nm He-Ne laser at 25 ^{o}C. The UV measurements of CC and FITC-CC were carried out at 408 and 495 nm, respectively. Circular dichroism (CD) spectra were recorded on a Jasco J-715 spectropolarimeter at 20 ^{o}C (Jasco PTC-348 WI peltier thermostat).

2.3. Synthesis of dPGA-FPBA

dPG with 90% amine functionalities (dPGA) was synthesized by a published three-step procedure.[25,26] FPBA (151.8 mg, 1.01 mM) and dPGA (1 g, 0.175 mM) were dissolved in 20 ml methanol in a round-bottom flask and the mixture was stirred overnight under argon atmosphere, which was followed by the addition of three equivalents $NaBH_4$ (114.5 mg, 3.03 mM) to reduce the imine bond. The pure product (FPBA functionality 5%, conversion 75.1%, yield 72.5%) was obtained by lyophilization after extensive dialyzing against distilled water (molecular weight cut-off 2000 Da). ^{1}H NMR (400 MHz, D_2O, 25 ^{o}C): δ = 2.48-3.18 (-C*H*$_2$-NH_2 or –C*H*-NH_2), 3.33-4.18 (dPG backbone), 7.11-7.53 (4H, ArH).[27]

2.4. Synthesis of dPGA-FPBA-CA

dPGA-FPBA (500 mg, 5.74 mmol of primary amine) was dissolved in pyridine (10 ml) and a certain amount of citraconic anhydride (CA) was added dropwise into the solution. The reaction was stirred overnight at room temperature, and then 1 M $NaHCO_3$ solution (50 ml) was poured into the solution. The compound was purified with Amicon Ultra filter (3 kDa MWCO, Millipore) by centrifuging it 4 times in $NaHCO_3$ solution and 3 times in distilled water. The pure conjugate with respectively 35%, 50%, and 65% CA functionalities was yellow powder after lyophilization. ^{1}H NMR (400 MHz, D_2O, 25 ^{o}C): δ = 5.51-5.90 (1H, CO*CH*CH_3COONa), 1.88-2.04 (3H, COCHCC*H*$_3$COONa).

2.5. Synthesis of nanogel (NGCA) by inverse nanoprecipitation

10 mg of dPGA-FPBA-CA was dissolved in 1 ml Milli-Q-water and 4 ml of dPG (10 mg/ml) aqueous solution was added. The mixture was injected into 200 ml acetone in a 500 ml round-bottom flask under intensive stirring, forming turbid solution. As soon as the mixture was homogeneous, the stirring was stopped and the in situ gelation was performed overnight at room temperature. The NGCA was purified by evaporating acetone and then ultrafiltrating with Amicon Ultra filter (10 kDa MWCO, Millipore) 4 times in Milli-Q-water. After lyophilization, the pure NGCA was obtained.

2.6. Preparation of CC-loaded nanogel (NGCA-CC)

20 mg of CC was added to 5 ml aqueous solution containing 10 mg dPGA-FPBA-CA with different CA functional percentages and 40 mg dPG. The mixture was immediately injected into 200 ml acetone with intensive stirring, followed by 24 h

immobilization. Acetone was evaporated and the residue was ultrafiltrated with Amicon Ultra filter (100 kDa MWCO, Millipore) 5 times in Milli-Q-water in order to remove the free CC. NG-65%CA-CC, NG-50%CA-CC, and NG-35%CA-CC were obtained by lyophilization and the loading capacity of CC was examined by UV-vis at 408 nm.[28] FITC-labeled CC (CC-FITC) was loaded into the nanogel following the same procedure.

2.7. pH-induced charge conversion and citraconic amide hydrolysis

To explore the pH-induced first-stage charge conversion of the zwitterionic nanogel, the zeta potential was measured at different pH values in the process of pH titration. 16 mg NGCA-CC with different percentages of CA moieties was respectively dispersed in 8 ml of PBS solution at pH 10.5 adjusted by NaOH solution. 0.1 and 0.01 M HCl solutions were used to titrate the substances, and the zeta potentials were measured at various pH values by a Zetasizer Nano-ZS (Malvern, UK).

To examine the hydrolysis of citraconic amide at different pH values, 10 mg NGCA was suspended in 10 ml of PBS at pH 7.4 or acetate buffer at pH 5 at 37 ^{o}C. At different time intervals, 1 ml of each nanogel suspension was subjected to the zeta potential measurement by a Zetasizer Nano-ZS (Malvern, UK).

2.8. ATP/pH-triggered degradation of NGCA

10 mg NGCA was homogeneously suspended in 10 ml different buffer solutions and incubated in a water bath at 37 ^{o}C under continuous stirring. The size changes over time were measured by DLS.

2.9. Protein release study

1 ml of NGCA-CC suspension (10 mg/ml) in PBS solution (pH 7.4) was transferred to a dialysis tube (molecular weight cut-off 300 kDa) and immersed into 30 ml of different release medium solutions at 37 ^{o}C with continuous stirring (200 rpm). At predetermined time intervals, 5 ml of release medium was taken out and replenished with an equal amount of fresh medium. The absorbance of CC was detected by UV-vis spectrophotometer at 408 nm for quantification. The release experiments were performed in triplicate, and the results represented a mean value with standard deviations. The released CC was collected and lyophilized. CD spectroscopy was conducted to measure the conformational change of the released CC compared to the free CC at a concentration of 0.5 mg/ml over the wavelength range from 190 to 240 nm.

2.10. Cytotoxicity

The MTT assay was used to evaluate the cell toxicity. MCF-7 cells were seeded into 96-well plates at 5000 cells per well and incubated for 24 h. Afterwards, the cell culture medium was removed and replaced with 100 μl supplemented RPMI containing NGCA, NGCA-CC, and free CC at pre-determined concentrations. After 48 h incubation, 10 μl of MTT solution (5 mg/ml in PBS) was added into each well and the cells were further incubated for 2 h. Then the culture medium was completely

removed and 100 μl of DMSO was added to dissolve the purple formazan crystals. The absorbance was determined by a microplate reader at the wavelength of 570 nm. The untreated cells were used as a control and the results were reported as the mean value of triplicate experiments with standard deviations.

The effect of pH on the cell proliferation inhibition of NGCA-CC was evaluated by MCF-7 cells with the similar procedure to the above. In brief, MCF-7 cells were seeded in 96-well plates (5000 cells/well). After 24 h incubation, the culture medium was replaced with 100 μl supplemented RPMI at pH 7.4 or 6.5 respectively containing NGCA-CC and CC at the CC concentration of 150 and 200 μg/ml. The cells were incubated for 1 h, and then the medium was replaced by 100 μl of fresh medium at neutral pH. MTT assay was generated after further incubation for 47 h.

2.11. Real-time cell analysis (RTCA)

The RTCA assay was conducted to dynamically monitor the cell proliferation and viability based on the Real-Time Cell Electronic Sensor (RT-CES) system. The cells were cultured in the microelectrode-coupled microtiter plates and the electrode impedance reflected the cell number, cell morphology, and the degree of cell adhesion.[29-32] The cells without treatment attached to the bottom of the well and enhanced the impedance, thereby inducing the increased cell index (CI) value. 50 μl of supplemented RPMI was added to each well of the E-plate (Roche, Mannheim, Germany) for background measurements. Then MCF-7 cells were added into the sensor wells at a concentration of 5000 cells per well for 24 h incubation, followed by replacing the culture medium with NGCA-CC and CC containing fresh medium at different concentrations. The E-plate was incubated for 48 h and monitored on the RTCA SP system (Roche, Mannheim, Germany) with time intervals of 15 min. The RTCA software version 2.0 was used for analysis. The cell proliferation inhibited by NGCA-CC at different pH values was monitored by RTCA device with the similar procedure as discussed in Section 2.9.

2.12. Cellular uptake

MCF-7 cells were seeded at the concentration of 1×10^5 cells per well in a 24-well plate with coverslips on the bottom of the wells. After 24 h incubation, the medium was replaced with fresh cell culture medium containing FM 4-64 (10 μg/ml) and CC or NGCA-CC, where CC was labeled with FITC, at a final CC concentration of 50 μg/ml. Additional 4 h and 24 h incubation was performed before removing the medium and rinsing trice with PBS solution. After being fixed with 4% paraformaldehyde PBS solution for 20 min, the cell nuclei were stained with DAPI for 30 min, followed by dryness. To investigate the effect of pH on the cellular uptake of NGCA, the cells were incubated in the CC or NGCA-CC containing culture medium with FM 4-64 (10 μg/ml) at pH 7.4 or 6.5, respectively. After 1 h, the cells were rinsed with PBS solution, which was followed by fixation and staining. The coverslips were pasted on the microscope slides and examined with a CLSM (Leica, Germany).

Flow cytometry was performed to quantify the cellular uptake. MCF-7 cells were

cultured in a 24-well plate at the density of 1×10^5 cells per well for 24 h. Then the medium was removed and replenished with substance-containing fresh medium at pH 7.4 and 6.5. After 1 h, the cells were washed trice with PBS solution after removing the culture medium, followed by harvesting with trypsin. The cells were fixed by 4% paraformaldehyde solution and resuspended in PBS supplemented with 1% fetal calf serum and 0.1% sodium azide. The fluorescence was quantitatively measured by a FACScalibur (Becton Dickinson, Heidelberg, Germany).

2.13. Cell apoptosis

The cell apoptosis induced by NGCA-CC and free CC was evaluated with a Dead Cell Apoptosis Kit (Lifetechnology, Germany). MCF-7 cells were cultured in a 24-well plate at a concentration of 1×10^5 cells per well for 24 h, and then treated with NGCA, free CC, and NGCA-CC, respectively. After a certain time point, the cells were harvested and washed with cold PBS twice, followed by suspension in 100 μl of binding buffer. 5 μl of Annexin V-Alexa Fluor®488 and 1 μl of PI (100 μg/ml) solutions were respectively added into the cell suspensions for 15 min incubation at room temperature under dark conditions. Then 300 μl of binding buffer was added and the cells were immediately analyzed with a FACScalibur (Becton Dickinson, Heidelberg, Germany). A 20 mW blue laser emitting at 488 nm served as the excitation source for Annexin V-Alexa Fluor®488 (FL1) and PI (FL2). Annexin V (green) and PI (red) fluorescent signals were collected at 530 nm and 610 nm pass filters, respectively, for 1×10^4 cells.

3. Results and discussion

3.1. Preparation of NGCA and NGCA-CC by inverse nanoprecipitaion

Scheme 1 shows the fabrication of NGCA and NGCA-CC. dPG was converted to 90% functionalized dPGA according to a three-step procedure published previously.[25,26] Then FPBA was conjugated with amine groups by a Schiff-base reaction, followed by the reduction with $NaBH_4$. The dPGA-FPBA conjugate was obtained with the secondary amino groups in the ortho position of a phenyl ring. The dative boron-nitrogen interaction (red arrow in Scheme 1) can improve the stability of the boronate ester under physiological conditions.[26] Afterwards, citraconic anhydride (CA) was coupled with some of the remaining amines in dPGA-FPBA to form an amide bond that is stable under neutral or basic conditions, but cleavable at acidic pH. dPGA-FPBA-CA with 35%, 50%, and 65% CA functionalities, respectively, were obtained as macromolecular crosslinkers.

The charge conversional nanogels were generated by using dPG as the main scaffold and dPGA-FPBA-CA as the crosslinker via a surfactant-free inverse nanoprecipitation method.[26,33,34] As shown in Scheme 1, the crosslinking occurred through the complexation of 1,2-diols in dPG and boronic acids in dPGA-FPBA-CA. The zwitterionic nanogels (NGCA) were formed with both positively charged amino groups and negatively charged carboxyl groups.

The therapeutic protein, cytochrome C (CC), was co-precipitated with the macromolecular precursors and encapsulated into the nanogels via an electrostatic

interaction between the cationic protein and anionic carboxyl groups in the nanogels. The loading capacity of CC was determined by UV-vis as 6.5%, 21%, and 25% for NG-35%CA-CC, NG-50%CA-CC, and NG-65%CA-CC, respectively.

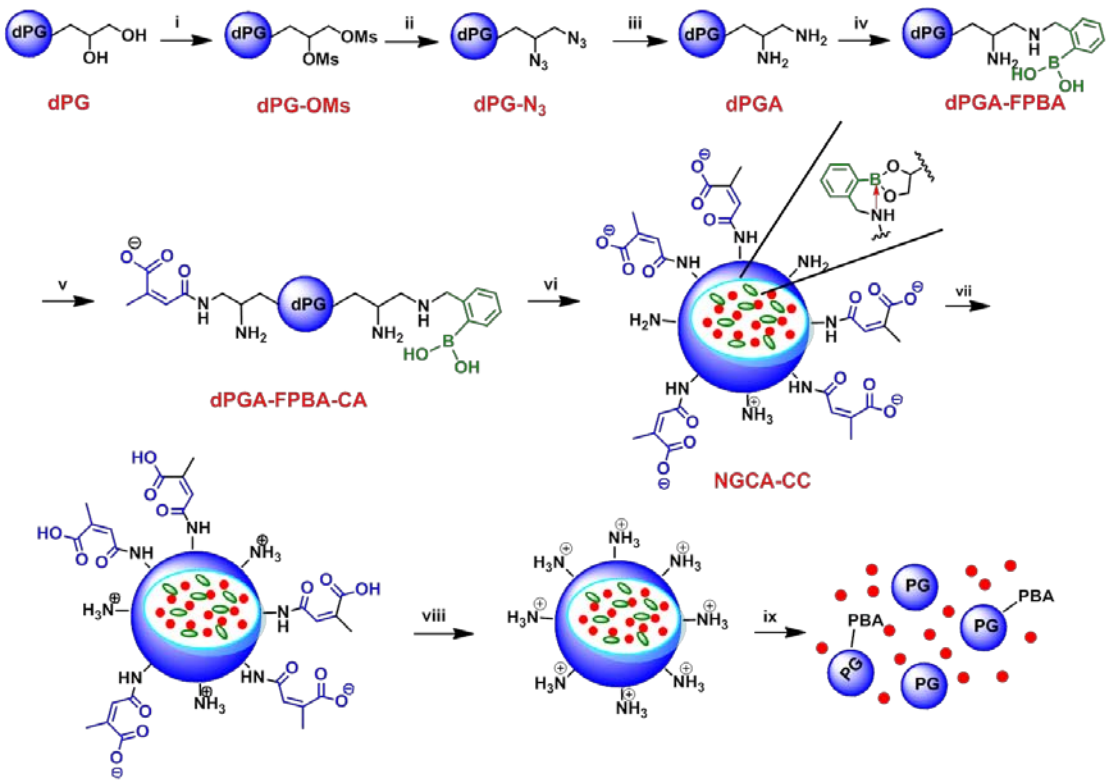

Scheme 1. Synthetic pathway of NGCA-CC: (i) Methanesulfonyl chloride (MsCl), pyridine, 0 ^{o}C to r.t., 16 h, (ii) NaN_3, 65 ^{o}C, 3 d, (iii) Triphenylphosphine (PPh_3), THF/H_2O, 24 h, (iv) FPBA, methanol, (v) $NaBH_4$, (vi) citraconic anhydride, pyridine, r.t., (vii) dPG, CC, inverse nanoprecipitation, (viii) pH 6.5, (ix) pH 5, (x) ATP.

3.2. pH-induced two-stage charge conversion

To demonstrate the charge conversional properties of the zwitterionic NGCA-CC according to the environmental pH, the zeta potential of NGCA-CC with different CA loadings was measured at various pH values by titration. As shown in Figure 2A, the zeta potentials of all the nanogels were negative at the starting pH of 10.5 and became gradually positive over titration with HCl solution due to the protonation of amino and carboxyl groups. The isoelectric points were 8.5, 7, and 5.8 for NG-35%CA-CC, NG-50%CA-CC, and NG-65%CA-CC, respectively. At tumor extracellular pH (6.5-6.8),[35] NG-50%CA-CC was capable of charge conversion and presented a slightly positive charge, which could promote the tumor cellular uptake. Therefore, all the following experiments were performed with NG-50%CA-CC (abbreviated as NGCA-CC).

Other than the zwitterionic conversion induced by protonation/deprotonation, the hydrolysis of citraconic amide at endosomal/lysosomal pH (5-6)[36] can cause the second stage charge conversion that is favorable for endosomal escape. Since CC cannot be stably retained inside the nanogel at pH 5 under 37 ^{o}C (see Section 3.4),

NGCA without CC entrapment was used to perform the hydrolysis study. As shown in Figure 2B, NGCA remained negatively charged during the whole period of measurement at pH 7.4, which is attributed to the relative higher stability of citraconic amide at neutral condition. At pH 5.0, NGCA had an initial negative surface charge of about –5 mV, whereas it reversed to positive within 2 h and continuously increased to the zeta potential of more than +20 mV. This was ascribed to the cleavage of citraconic amide bond, resulting in the exposure of amine groups, which was also proven by the ^{1}H NMR (Figure S1) and ninhydrin reaction (Figure S2).

As illustrated in Figure 2C, NGCA-CC is negatively charged at blood pH (7.4), but becomes positive under tumor tissue pH (6.5), facilitating cellular uptake. After internalization into the tumor cells, the positive charge of NGCA-CC is further increased in the endosome (pH 5) induced by the cleavage of citraconic amide, which promotes endosomal escape.

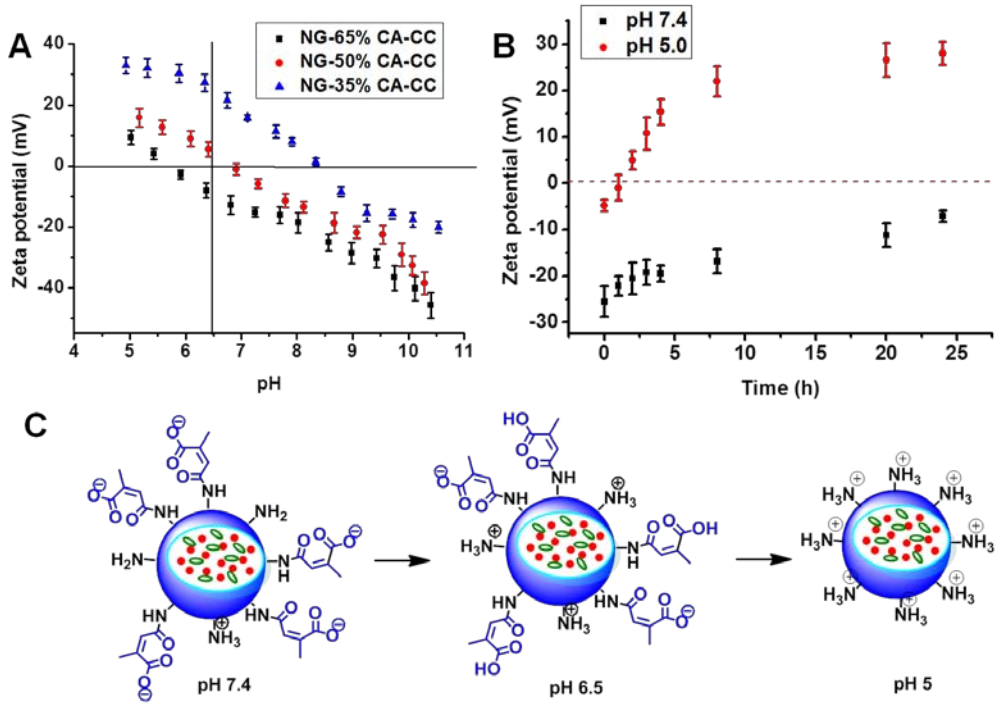

Figure 2. (A) The change of zeta potential for NGCA-CC with different CA functionalities over pH by pH titration; (B) the change of zeta potential for NGCA over time at pH 7.4 and 5.0; (C) schematic illustration of the two-stage charge conversion of zwitterionic nanogels.

3.3. Degradation of NGCA

The degradation behavior of NGCA was detected by DLS. In the presence of 5 mM ATP (Figure 3A), NGCA swelled after 1 h due to the partial cleavage of boronate ester crosslinkages caused by the competitive binding of ATP with boronic acid. After 24 h, NGCA was completely dissociated into precursors. As shown in Figure 3B, NGCA only swelled due to the partial cleavage of boronate ester at pH 5 after 24 h, which is in accordance with our previously published results.[26]

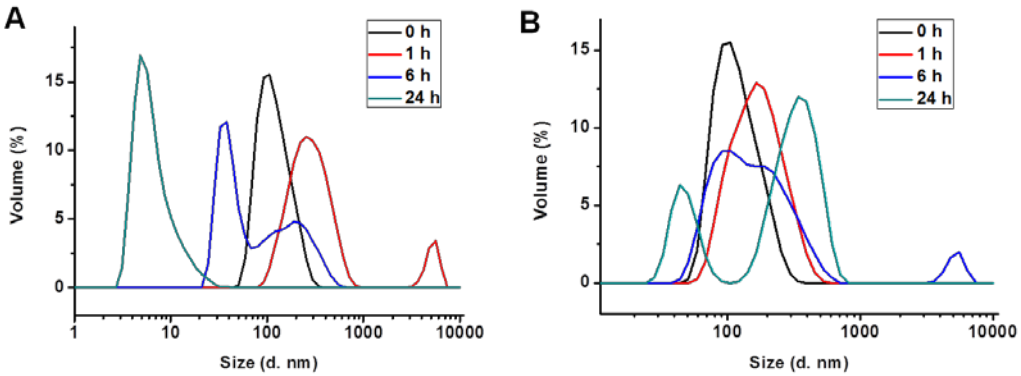

Figure 3. Degradation of NGCA determined over time with DLS (A) in the presence of 5 mM ATP at pH 7.4 and (B) at pH 5.

3.4. In vitro protein release

Figure 4 shows the release profiles of CC from NGCA-CC under different conditions. ATP and pH gradients between intracellular and extracellular environment are both important biological signals. At tumor extracellular pH (6.5), the release of CC was faster than that at pH 7.4. By lowering the pH, the electrostatic interaction between cationic CC and the anionic nanogel decreased because of the protonation of amino and carboxyl groups in the nanogel. When the pH decreased to 5, the boronate ester bond started to degrade, which induced the swelling of the nanogel and accelerated the CC release. In the intracellular ATP mimicking environment (5 mM ATP solution at pH 7.4), CC was released significantly faster compared to physiological conditions (pH 7.4). It has been reported that ATP can dissociate the boronate ester crosslinkers of the nanogel scaffold by competing with dPG.[26] The protein-loaded nanogels were prepared under mild conditions, which were not supposed to lead to protein denaturation or deactivation. CD analysis showed that the released CC possessed a similar profile to the native CC in the range from 200 to 240 nm (Figure S4), indicating that the secondary structure of CC was retained during encapsulation and release.

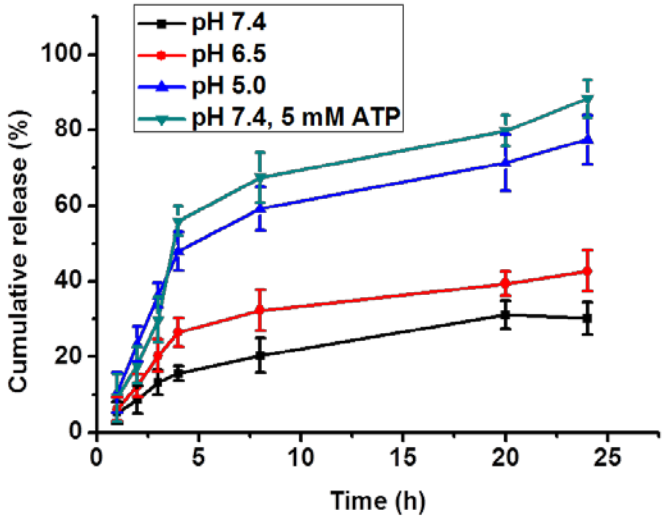

Figure 4. Release profiles of CC in buffer solutions with different pH or in the presence of 5 mM ATP.

3.5. In vitro cytotoxicity

The cytotoxicity of NGCA-CC and free CC were investigated by MTT assay (Figure 5A). Free CC caused a limited decrease in the cell viability and treatment with NGCA-CC induced a dose-dependent reduction of the cell viability. Since the MTT test did not show any obvious toxicity of NGCA towards MCF-7 cells up to a concentration of 1 mg/ml (Figure S5), the cell death was caused by the uptake and intracellular release of CC. A more detailed investigation about dose-dependent cytotoxicity was performed by RTCA (Figure S6), which presented consistent results with the MTT assay.

We further studied the influence of environmental pH on the antitumor activity of NGCA-CC. As shown in Figure 5B, NGCA-CC showed an obviously enhanced antitumor activity at pH 6.5 compared to that at pH 7.4. At pH 6.5, charge conversion rapidly occurred as discussed in Section 3.2 (Figure 2A) and produced positively charged NGCA-CC that should have exhibited a higher cellular uptake than the negative nanogel particles at pH 7.4. Free CC did not induce any toxicity on MCF-7 cells at both pH conditions. The RTCA analysis in Figure 5C also demonstrated a stronger inhibition of cell proliferation induced by NGCA-CC at pH 6.5 than pH 7.4.

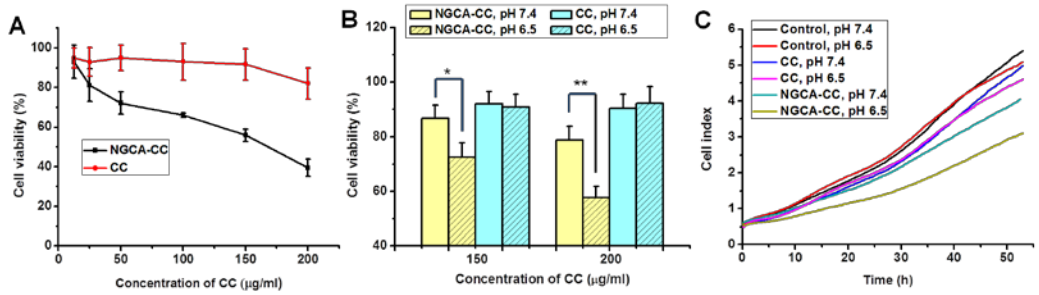

Figure 5. (A) In vitro cytotoxicity of NGCA-CC and free CC towards MCF-7 cells determined by MTT assay at various CC concentrations for 48 h; in vitro cytotoxicity treated with substances at pH 7.4 or 6.5 for 1 h and further incubated in the fresh medium for 47 h by (B) MTT assay and (C) RTCA measurements. The untreated cells were set as a control. Data presented as the average ± standard deviation (Student's t-test, n = 4, *p < 0.05, **p < 0.01).

3.6. pH-dependent cellular uptake and intracellular protein release

In order to examine the influence of the charge conversional property on the tumor cellular uptake, MCF-7 cells were incubated respectively with NGCA-CC and free CC at pH 7.4 or 6.5 for 1 h. A red fluorescent endosome marker, FM 4-64, was used to stain the endosomes. CC was labeled with FITC according to the reported procedure.[37] As shown in Figure 6, the cellular uptake of NGCA-CC was higher at pH 6.5 than 7.4, demonstrating a pH-dependent uptake process of the nanogel. The enhanced cellular uptake at tumor extracellular condition (pH 6.5) was ascribed to the

electrostatic absorption between the negatively charged cell membrane and the positively charged nanogels. In comparison, the uptake of free CC showed negligible change. In Figure S7, the quantitative internalization by flow cytometry was in accordance with the CLSM results. The charge conversion of NGCA-CC was an instantaneous process and a prompt response to pH change, unlike the relatively slower DMMA cleavage with its reaction time for the amide degradation.[38,39]

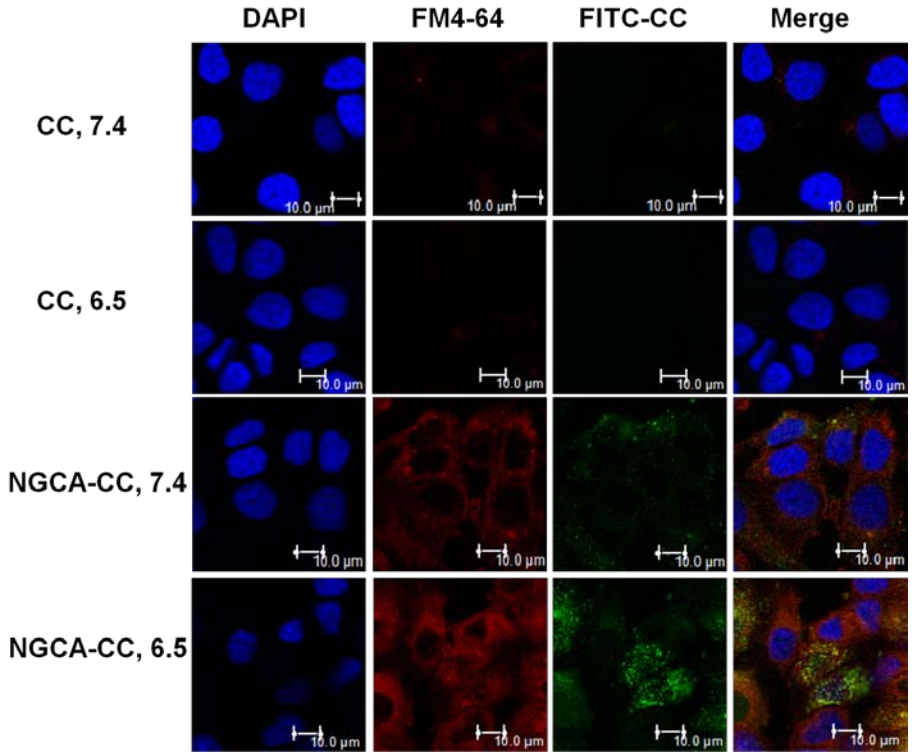

Figure 6. CLSM images of MCF-7 cells after the treatment of free CC or NGCA-CC, where CC is labeled with FITC, for 1 h at pH 7.4 or 6.5. The nuclei were stained with DAPI (blue) and the endosomes were stained with FM4-64 (red).

To determine whether or not the NGCA-CC could escape from the endosomal compartments, the cells were cultured in the substance-containing medium for 4 h and 24 h before measurement. In Figure 7, free CC showed negligible internalization at both time points. In comparison, a co-localization of NGCA-CC and endosomes, represented in yellow, was observed at 4 h. However, the green fluorescence of NGCA-CC showed an evident dissociation with the red fluorescence at 24 h (see enlarged images in Figure S8), which demonstrated their ability to endosomally escape. The probable reason is more amine groups can be exposed due to the cleavage of citraconic amide in the acidic endosomal environment, thus disrupting the endosomal membrane by the proton sponge effect.[40]

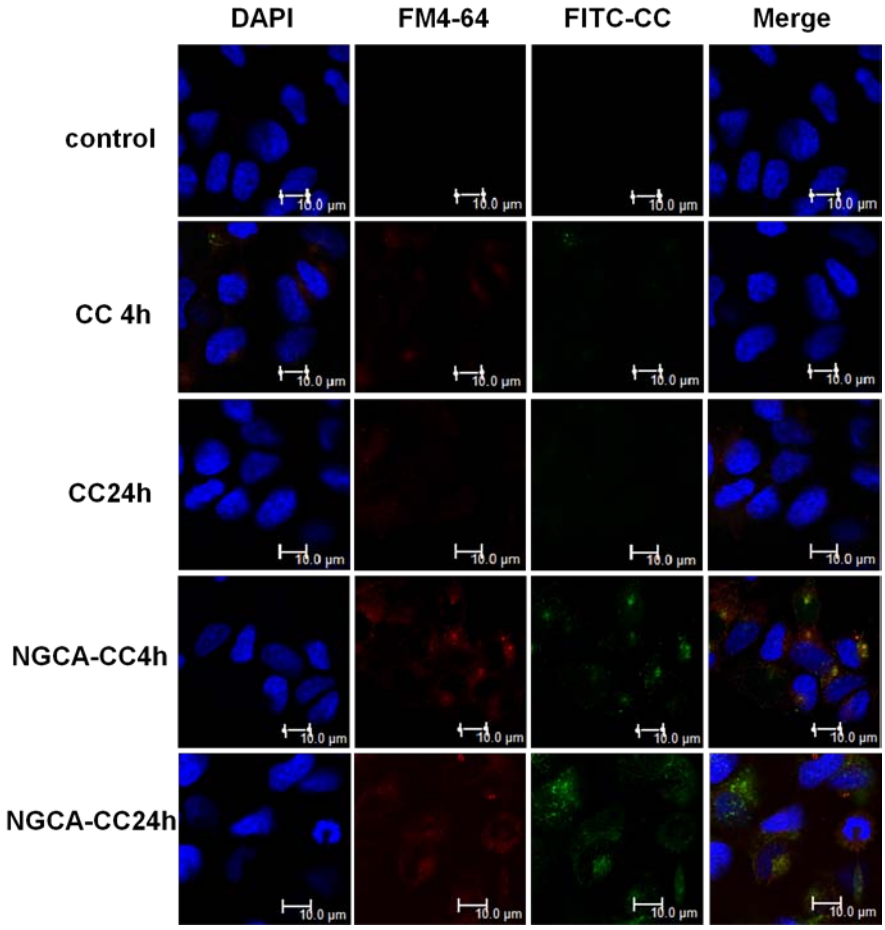

Figure 7. CLSM images of MCF-7 cells treated with free CC or NGCA-CC, in which CC was labeled with FITC, at 4 and 24 h. The nuclei were stained with DAPI (blue) and the endosomes were stained with FM4-64 (red).

3.7. Cell apoptosis

CC is a therapeutic protein that is able to induce programmed cell death by the mitochondria dependent apoptosis. The level of apoptosis was determined by annexin V-Alexa Fluor®488/PI staining using flow cytometry at a CC dosage of 50 μg/ml. NGCA did not induce higher cell apoptosis than the control even after 48 h treatment (Figure S9). Figure 8 shows the expression of annexin V and the permeation of PI in MCF-7 cells treated for 24 h with NGCA-CC and free CC, respectively. Quadrant 2 (Q2) showed the early apoptosis and quadrant 3 (Q3) represented the late apoptotic and necrotic cells. Only 13.8% (Q2+Q3) control cells exhibited apoptosis, whereas 27.8% apoptosis was induced by NGCA-CC. In contrast, much lower apoptosis was observed for free CC (18.5 %). Therefore, it is evident that the transfer of CC into cells was enhanced by the nanogel carriers so that it can more efficiently induce cell death by apoptosis.

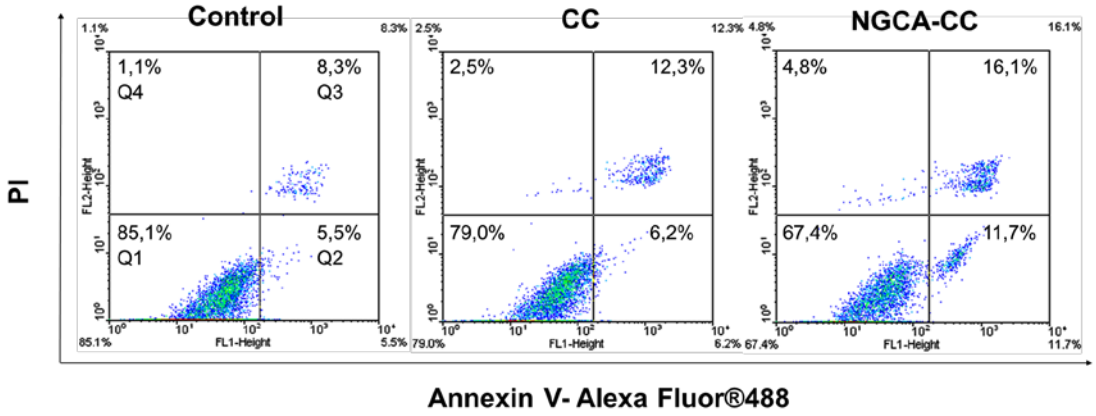

Figure 8. Contour diagram of Annexin V-Alexa Fluor®/PI flow cytometry of MCF-7 cells treated with free CC or NGCA-CC for 24 h with CC dosage of 50 μg/ml. ***Q1***: living cells. ***Q2*****:** early apoptotic cells. ***Q3*****:** late apoptotic and necrotic cells. ***Q4*****:** necrotic cells.

4. Conclusions

In conclusion, we designed and prepared a biodegradable zwitterionic nanogel with two-stage charge conversional properties for therapeutic protein delivery. The introduction of citraconic anhydride is, on the one hand, to provide carboxyl groups for complexing CC and offering the zwitterionic property for the first-stage charge conversion in the tumor extracellular environment, and, on the other hand, to form pH-cleavable citraconic amide that can release amino groups under the acidic organelle conditions for the second-stage charge conversion. Having escaped from the endosome, CC could be efficiently released due to the dissociation of nanogel in the ATP-containing cytosol, which resulted in cell death by mitochondria dependent apoptosis.

Acknowledgements

This study was supported by the Chinese Scholar Council (CSC), the focus area nanoscale of Freie Universität Berlin (www.nanoscale.fu-berlin.de), and the core-facility biosupramol (www.biosupramol.de). We thank Dr. Pamela Winchester for proofreading this manuscript, Dr. Katharina Achazi for the help with biological tests, Dr. Hua Fan for the support in flow cytometry experiments, and Florian Paulus for PG synthesis.

References

(1) Goeddel, D. V.; Kleid, D. G.; Bolivar, F.; Heyneker, H. L.; Yansura, D. G.; Crea, R.; Hirose, T.; Kraszewski, A.; Itakura, K.; Riggs, A. D. *PNAS* **1979**, *76*, 106-110.

(2) Lu, Y.; Sun, W.; Gu, Z. *J. Control. Release* **2014**, *194*, 1-19.

(3) Schrama, D.; Reisfeld, R. A.; Becker, J. C. *Nat. Rev. Drug Discov.* **2006**, *5*, 147-159.

(4) Nochi, T.; Yuki, Y.; Takahashi, H.; Sawada, S. I.; Mejima, M.; Kohda, T.; Harada, N.; Kong, I. G.; Sato, A.; Kataoka, N.; Tokuhara, D.; Kurokawa, S.; Takahashi, Y.; Tsukada, H.; Kozaki, S.; Akiyoshi, K.; Kiyono, H. *Nat. Mater.* **2010**, *9*, 572-578.

(5) Lee, K. Y.; Yuk, S. H. *Prog. Polym. Sci.* **2007**, *32*, 669-697.

(6) Lee, Y.; Ishii, T.; Cabral, H.; Kim, H. J.; Seo, J. H.; Nishiyama, N.; Oshima, H.; Osada, K.; Kataoka, K. *Angew. Chem. Int. Ed.* **2009**, *121*, 5413-5416.

(7) Cho, E. C.; Xie, J.; Wurm, P. A.; Xia, Y. *Nano Lett.* **2009**, *9*, 1080-1084.

(8) Gratton, S. E. A.; Ropp, P. A.; Pohlhaus, P. D.; Luft, J. C.; Madden, V. J.; Napier, M. E.; DeSimone, J. M. *PNAS* **2008**, *105*, 11613-11618.

(9) Muñoz Javier, A.; Kreft, O.; Piera Alberola, A.; Kirchner, C.; Zebli, B.; Susha, A. S.; Horn, E.; Kempter, S.; Skirtach, A. G.; Rogach, A. L.; Rädler, J.; Sukhorukov, G. B.; Benoit, M.; Parak, W. J. *Small* **2006**, *2*, 394-400.

(10) Ge, Z.; Liu, S. *Chem. Soc. Rev.* **2013**, *42*, 7289-7325.

(11) Lee, Y.; Fukushima, S.; Bae, Y.; Hiki, S.; Ishii, T.; Kataoka, K. *J. Am. Chem. Soc.* **2007**, *129*, 5362-5363.

(12) Lee, E. S.; Oh, K. T.; Kim, D.; Youn, Y. S.; Bae, Y. H. *J. Control. Release* **2007**, *123*, 19-26.

(13) Du, J. Z.; Sun, T. M.; Song, W. J.; Wu, J.; Wang, J. *Angew. Chem. Int. Ed.* **2010**, *122*, 3703-3708.

(14) Li, J.; Han, Y.; Chen, Q.; Shi, H.; ur Rehman, S.; Siddiq, M.; Ge, Z.; Liu, S. *J. Mater. Chem. B* **2014**, *2*, 1813-1824.

(15) Chen, W.; Achazi, K.; Schade, B.; Haag, R. *J. Control. Release* **2015**, *205,* 15-24.

(16) Meyer, M.; Philipp, A.; Oskuee, R.; Schmidt, C.; Wagner, E. *J. Am. Chem. Soc.* **2008**, *130*, 3272-3273.

(17) Du, J. Z.; Du, X. J.; Mao, C. Q.; Wang, J. *J. Am. Chem. Soc.* **2011**, *133*, 17560-17563.

(18) Tian, H.; Guo, Z.; Lin, L.; Jiao, Z.; Chen, J.; Gao, S.; Zhu, X.; Chen, X. *J. Control. Release* **2014**, *174*, 117-125.

(19) Mo, R.; Sun, Q.; Xue, J.; Li, N.; Li, W.; Zhang, C.; Ping, Q. *Adv. Mater.* **2012**, *24*, 3659-3665.

(20) Mo, R.; Sun, Q.; Li, N.; Zhang, C. *Biomaterials* **2013**, *34*, 2773-2786.

(21) Lee, Y.; Ishii, T.; Cabral, H.; Kim, H. J.; Seo, J. H.; Nishiyama, N.; Oshima, H.; Osada, K.; Kataoka, K. *Angew. Chem. Int. Ed.* **2009**, *48*, 5309-5312.

(22) Lee, Y.; Ishii, T.; Kim, H. J.; Nishiyama, N.; Hayakawa, Y.; Itaka, K.; Kataoka, K. *Angew. Chem. Int. Ed.* **2010**, *49*, 2552-2555.

(23) Sunder, A.; Mülhaupt, R.; Haag, R.; Frey, H. *Adv. Mater.* **2000**, *12*, 235-239.

(24) Sunder, A.; Hanselmann, R.; Frey, H.; Mülhaupt, R. *Macromolecules* **1999**, *32*, 4240-4246.

(25) Roller, S.; Zhou, H.; Haag, R. *Mol Divers* **2005**, *9*, 305-316.

(26) Zhang, X.; Achazi, K.; Haag, R. *Adv. Healthc. Mater.* **2015**, *4*, 585-592.

(27) Piest, M.; Ankoné, M.; Engbersen, J. F. J. *J. Control. Release* **2013**, *169*, 266-275.

(28) Ma, X.; Zhang, L. H.; Wang, L. R.; Xue, X.; Sun, J. H.; Wu, Y.; Zou, G.; Wu, X.; Wang, P. C.; Wamer, W. G.; Yin, J. J.; Zheng, K.; Liang, X. J. *ACS Nano* **2012**, *6*, 10486-10496.

(29) Ryder, A. B.; Huang, Y.; Li, H.; Zheng, M.; Wang, X.; Stratton, C. W.; Xu, X.; Tang, Y. W. *J. Clin. Microbiol.* **2010**, *48*, 4129-4134.

(30) Atienza, J. M.; Zhu, J.; Wang, X.; Xu, X.; Abassi, Y. *J. Biomol. Screen.* **2005**, *10*, 795-805.

(31) Solly, K.; Wang, X.; Xu, X.; Strulovici, B.; Zheng, W. *ASSAY Drug Dev. Techn.* **2004**, *2*, 363-372.

(32) Xing, J. Z.; Zhu, L.; Jackson, J. A.; Gabos, S.; Sun, X. J.; Wang, X. B.; Xu, X. *Chem. Res. Toxicol.* **2005**, *18*, 154-161.

(33) Zhang, X.; Achazi, K.; Steinhilber, D.; Kratz, F.; Dernedde, J.; Haag, R. *J. Control. Release* **2014**, *174*, 209-216.

(34) Steinhilber, D.; Witting, M.; Zhang, X.; Staegemann, M.; Paulus, F.; Friess, W.; Küchler, S.; Haag, R. *J. Control. Release* **2013**, *169*, 289-295.

(35) Rofstad, E. K.; Mathiesen, B.; Kindem, K.; Galappathi, K. *Cancer Res.* **2006**, *66*, 6699-6707.

(36) Zhang, X.; Malhotra, S.; Molina, M.; Haag, R. *Chem. Soc. Rev.* **2015**, *44*, 1948-1973.

(37) Slowing, I. I.; Trewyn, B. G.; Lin, V. S. Y. *J. Am. Chem. Soc.* **2007**, *129*, 8845-8849.

(38) Du, J. Z.; Sun, T. M.; Song, W. J.; Wu, J.; Wang, J. *Angew. Chem. Int. Ed.* **2010**, *49*, 3621-3626.

(39) Guo, X.; Shi, C.; Yang, G.; Wang, J.; Cai, Z.; Zhou, S. *Chem. Mater.* **2014**, *26*, 4405-4418.

(40) Varkouhi, A. K.; Scholte, M.; Storm, G.; Haisma, H. J. *J. Control. Release* **2011**, *151*, 220-228.

Supporting information

Multi-stage, charge conversional, stimuli-responsive nanogels for therapeutic protein delivery

Xuejiao Zhang[1,*], Kai Zhang[2], Rainer Haag[1]

1 Freie Universität Berlin, Institut für Chemie und Biochemie, Takustraße 3, 14195 Berlin, Germany
2 Charité-Universitätsmedizin Berlin, Institut für Laboratoriumsmedizin, Klinische Chemie und Pathobiochemie, 13353 Berlin, Germany

Corresponding author:
Xuejiao Zhang
Institute for Chemistry and Biochemistry
Freie Universität Berlin
Takustrasse 3, Berlin 14195 (Germany)
E-mail: zhangxuejiao1985@gmail.com

1. Cleavage of citraconic amide

1.1. ^{1}H NMR spectra

20 mg of NGCA was dispersed in 5 ml of acetate buffer solution at pH 5.0 for 8 h incubation. After lyophilization, the residue was dissolved in D_2O for proton NMR measurement.

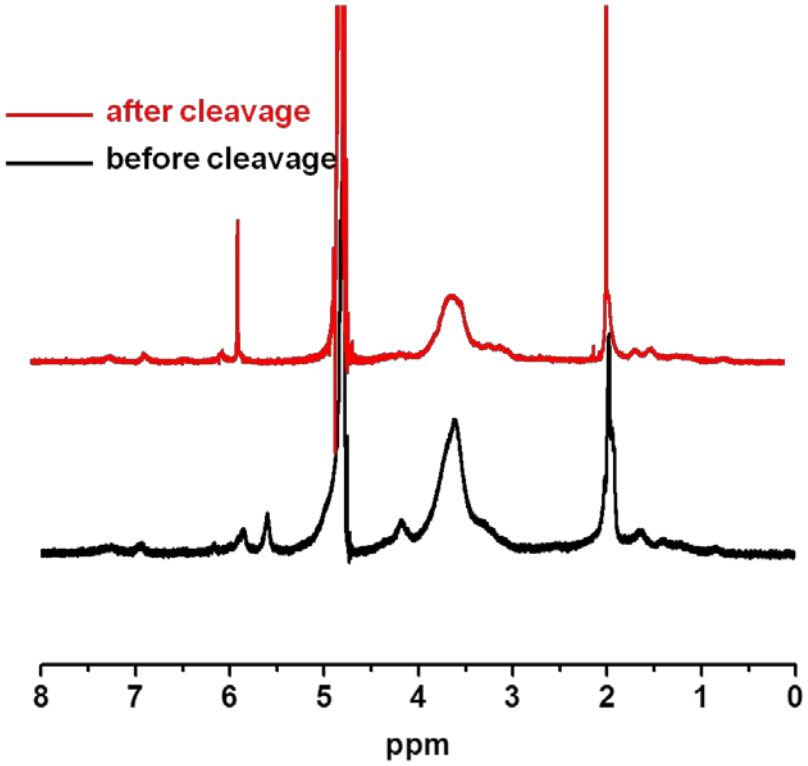

Figure S1. ^{1}H NMR spectra of NGCA before (black) and after (red) treatment at pH 5.

1.2. Ninhydrin assay

10 mg NGCA was incubated in 10 ml of PBS solution at pH 7.4 or acetate buffer solution at pH 5.0 at 37 ^{o}C. At pre-determined time points, the amount of primary amine was determined by Ninhydrin assay [1]. 90% exposed primary amine was determined by the fluorescence of NGCA after being incubated in HCl aqueous solution (pH 3) overnight.

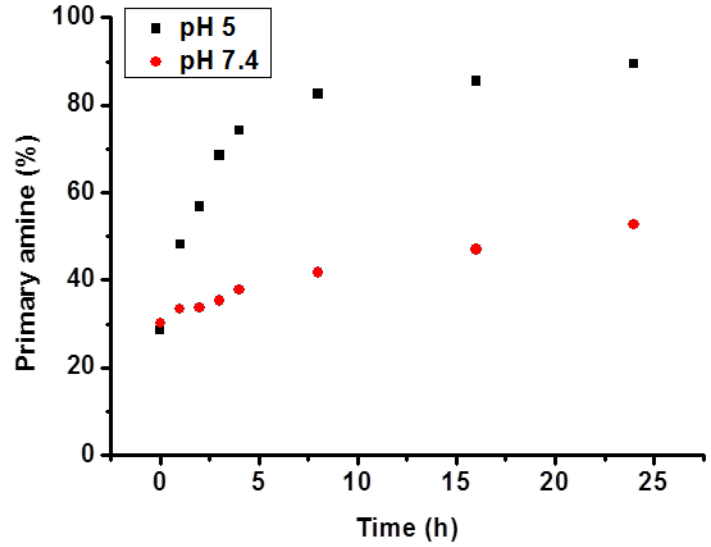

Figure S2. The citraconic amide degradation at pH 7.4 and 5.

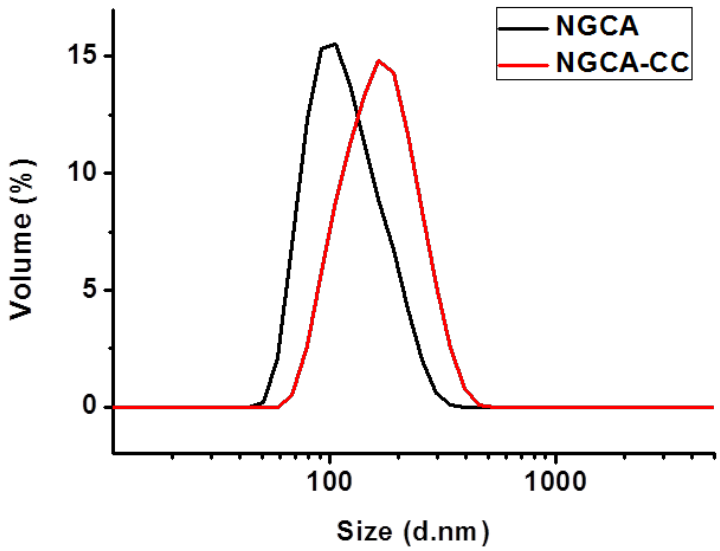

Figure S3. Size distribution of blank nanogel (NGCA) and protein loaded nanogel (NGCA-CC).

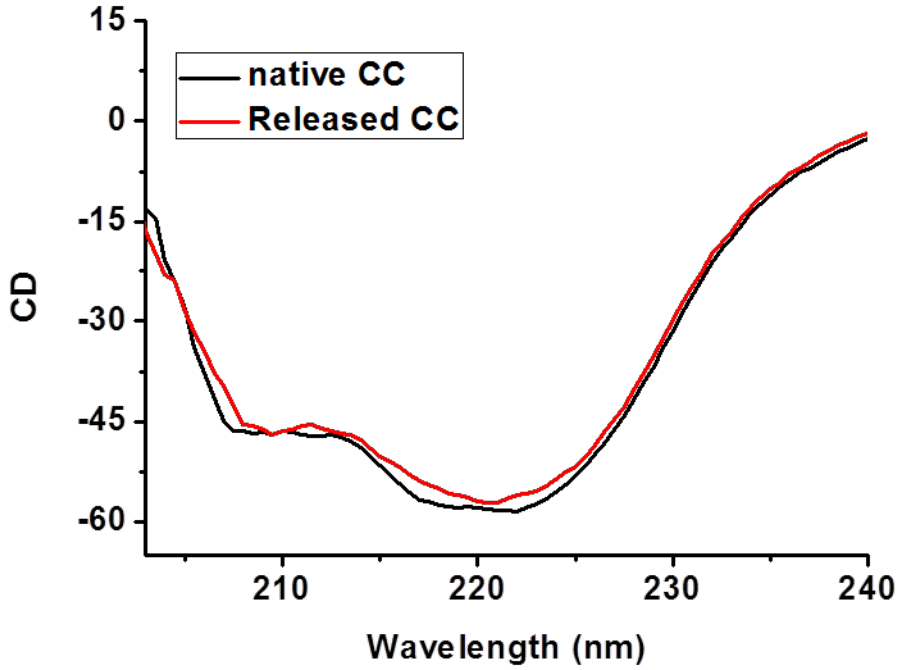

Figure S4. CD spectra of native CC and released CC at a concentration of 500 μg/ml.

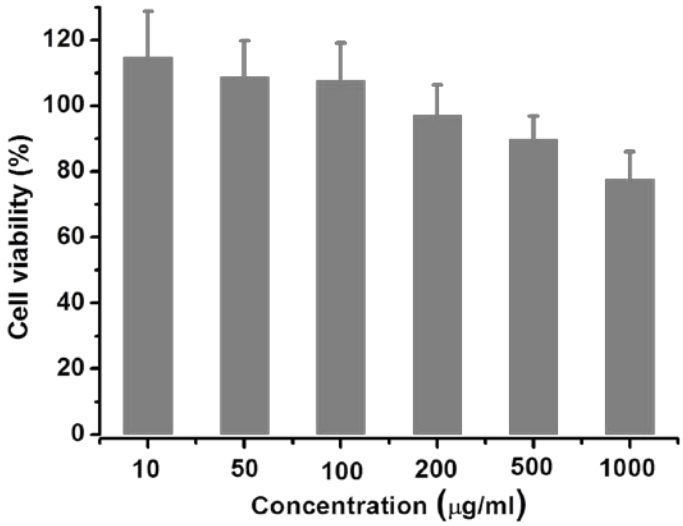

Figure S5. Cell viability of MCF-7 cells after the treatment of different concentrations of NGCA for 48 h. The cell viability of untreated control was set to 100%.

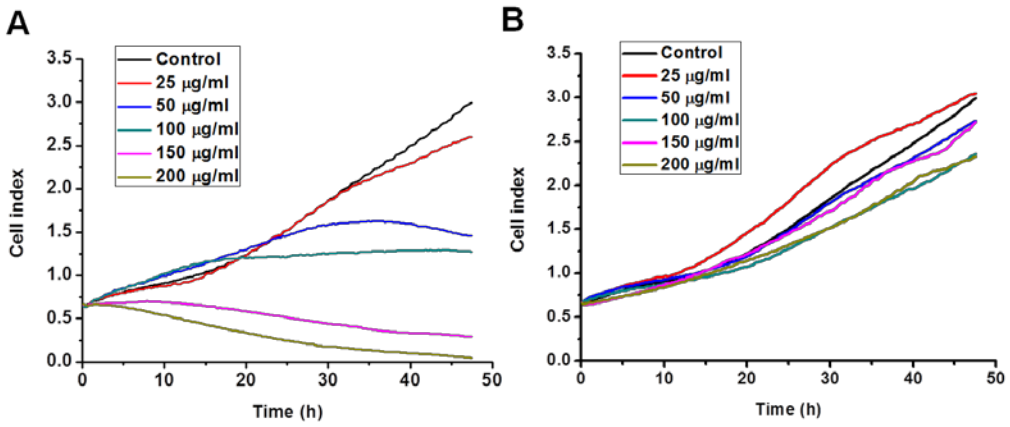

Figure S6. Cytotoxicity profiles of MCF-7 cells determined by an xCelligence RTCA device. Cell proliferation over time under the treatment of (A) NGCA-CC and (B) CC at different concentrations of CC.

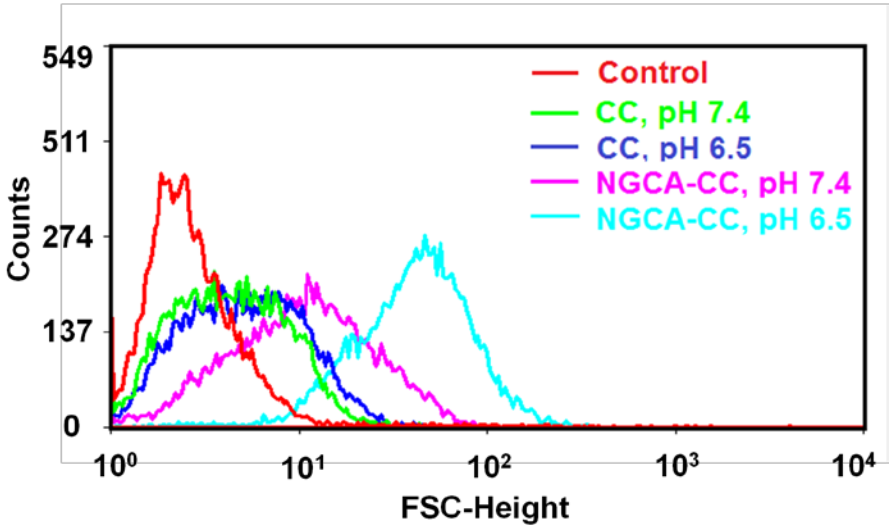

Figure S7. Flow cytometry profiles of MCF-7 cells treated with free CC or NGCA-CC for 1 h at pH 7.4 and 6.5.

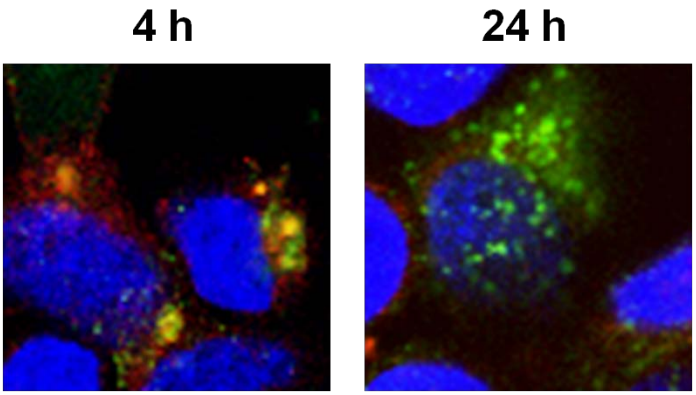

Figure S8. CLSM images of MCF-7 cells after 4 h and 24 h treatment with NGCA-CC.

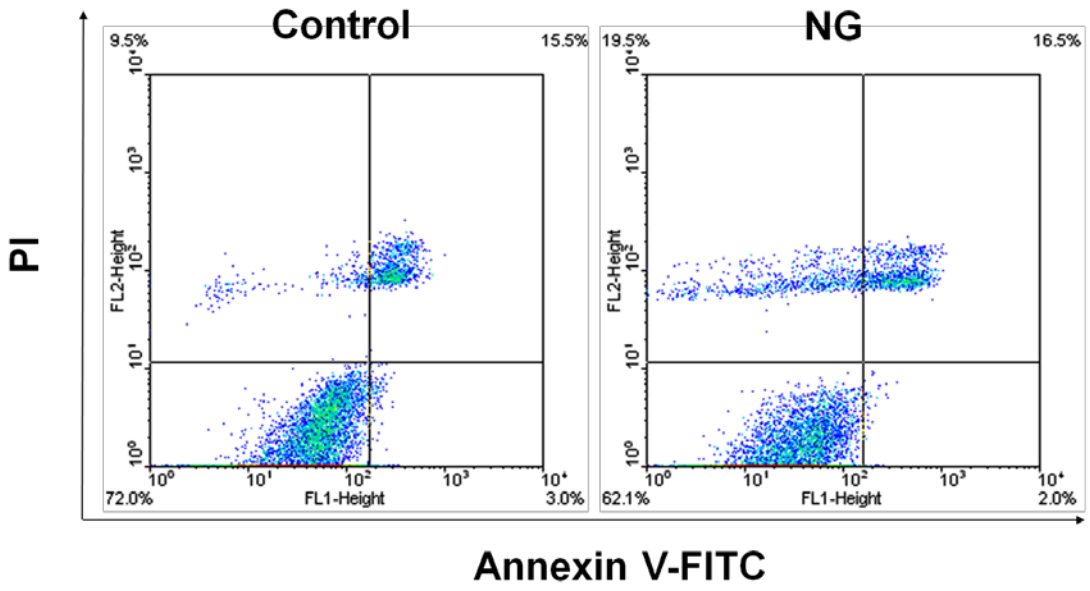

Figure S9. Contour diagram of Annexin V-FITC/PI flow cytometry of MCF-7 cells after 48 h treatment of NGCA-CC at a concentration of 500 μg/ml.

[1] Yemm EW, Cocking EC, Ricketts RE. The determination of amino-acids with ninhydrin. Analyst. 1955;80:209-14.

NMR spectra

dPG-90%NH_2 (dPGA)

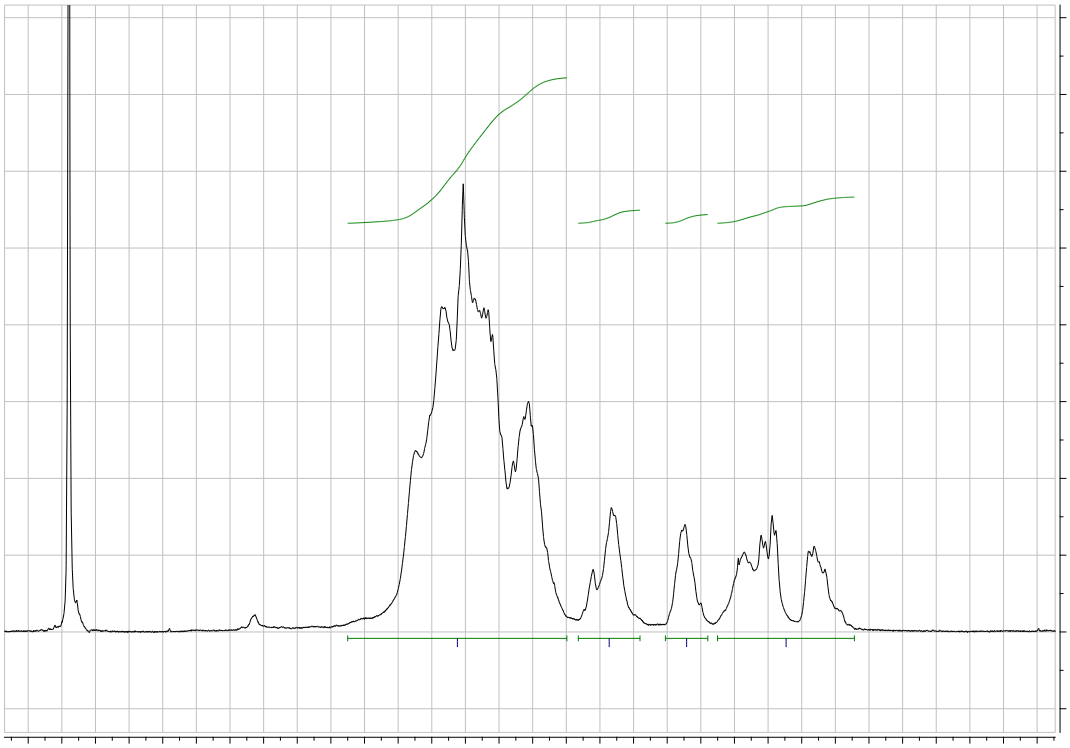

dPGA-5%FPBA

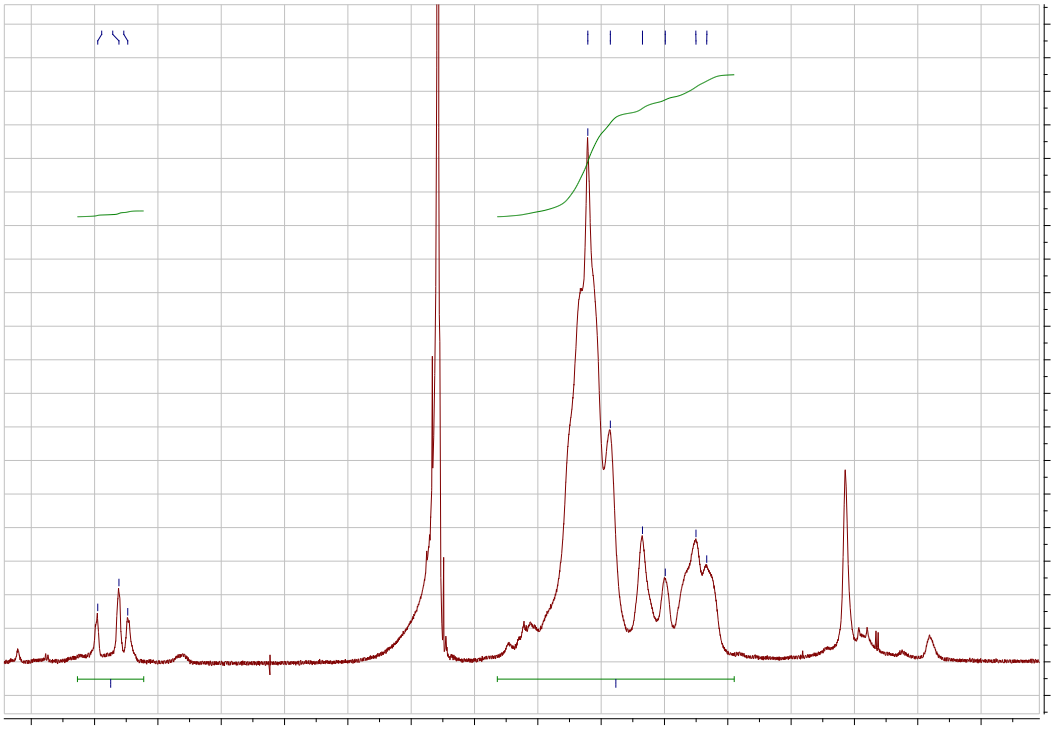

dPGA-5%FPBA-35%CA

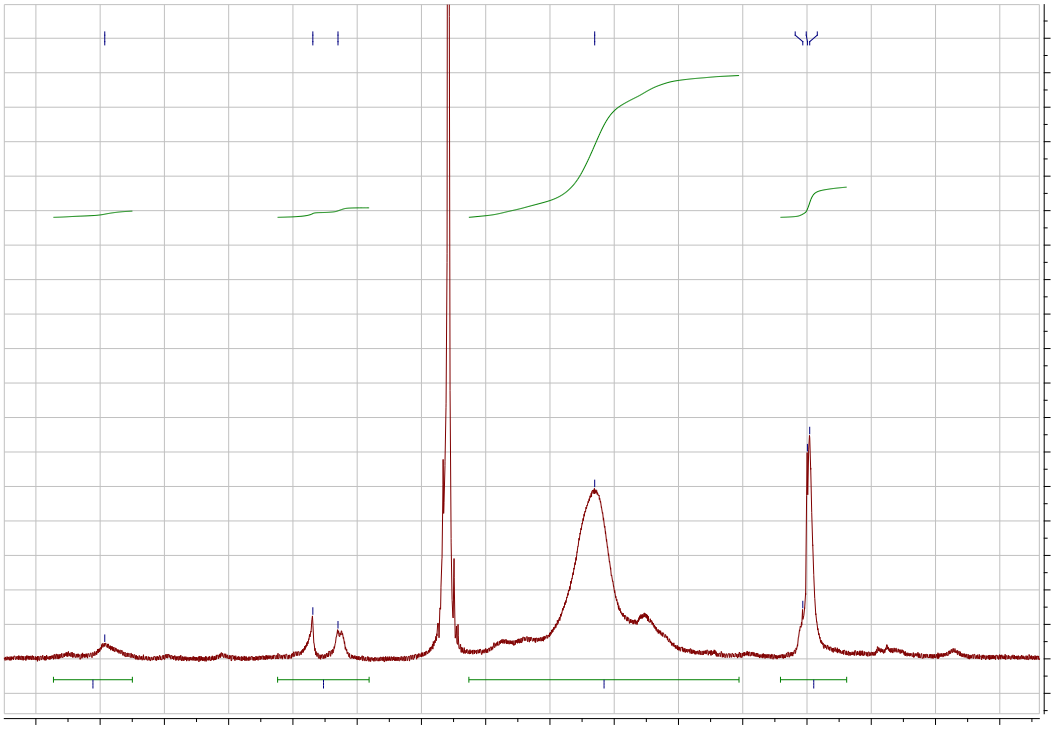

dPGA-5%FPBA-50%CA

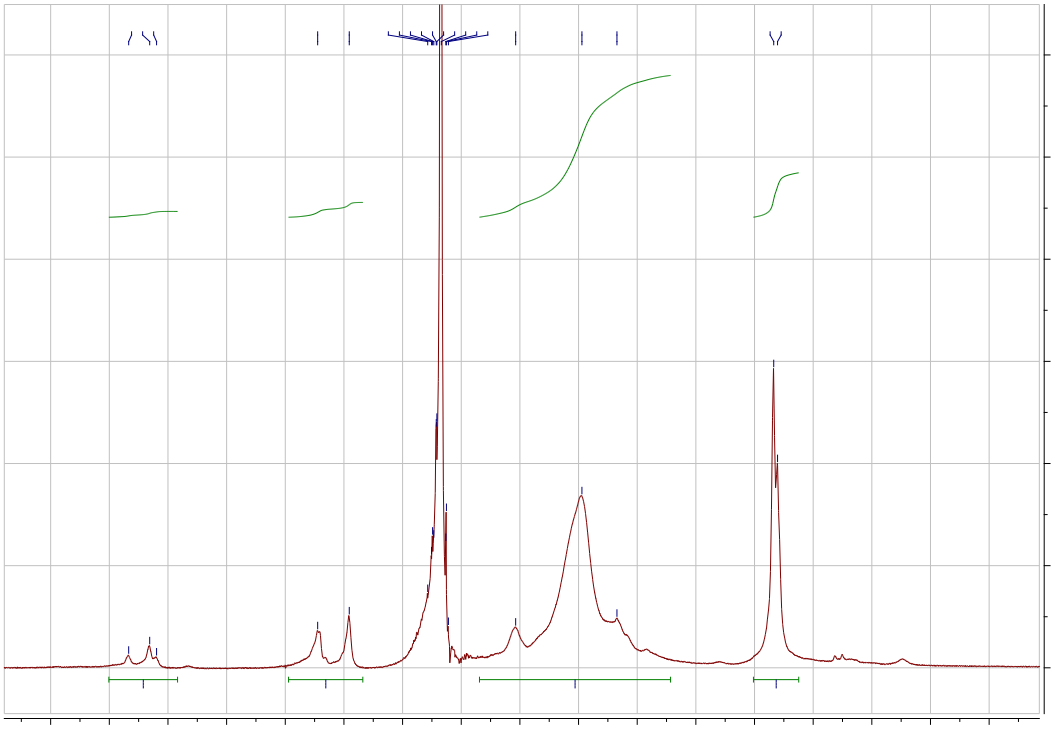

dPGA-5%FPBA-65%CA

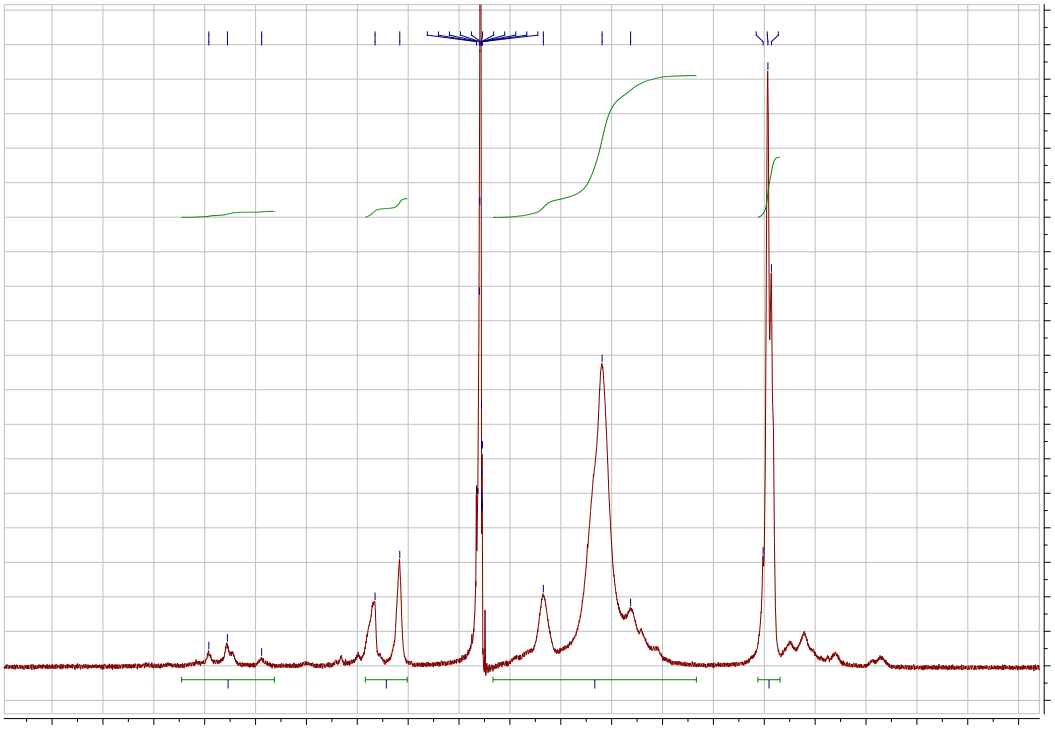

4. Summary and outlook

In this thesis, an inverse nanoprecipitation approach, which is mild, surfactant free, and low energy consuming, has been applied to fabricate biodegradable nanogels based on a dendritic polyglycerol (dPG). A series of dPG-based macromolecular precursors were synthesized and the corresponding nanogel particles with tunable dimensions and narrow dispersity were generated in the process of in situ gelation via inverse nanoprecipitation. The obtained nanogels are promising candidates for the delivery of anticancer drugs and proteins due to their highly biocompatible scaffold. They were capable of transporting the guest molecules into cells and releasing them in response to the intracellular signals.

In order to make use of multiple intracellular signals, a dual-responsive nanogel system with both pH and redox sensitivity was prepared by the thiol-disulfide exchange reaction. Thioctic acid functionalized dPG was synthesized as the macromolecular precursor, and a deficient amount of dithiothreitol (DTT) was used to cleave the lipoyl ring to the corresponding dihydrolipoyl groups that initiated the thiol-disulfide exchange reaction. The disulfide crosslinked network was degradable under intracellular redox conditions, thus producing small degradation fragments that could be cleared from the body. DOX was covalently conjugated with an acid labile hydrazone linker, which is stable under physiological conditions but cleavable in the acidic cell organelles. The prodrug nanogels can efficiently enter into tumor cells, release the drug in response to the intracellular environment, and ultimately induce the cell death.

Another important intracellular signal is the higher concentration of ATP in cytosol compared to the extracellular environment. We designed a new ATP and pH dual-responsive degradable nanogel crosslinked with boronate ester bonds between 1,2-diols in dPG and boronic acid for the intracellular delivery of anticancer drugs. MTX was encapsulated by electrostatic interactions and can be rapidly released upon the treatment with ATP or acidic conditions. The nanogels could swell under organelle

pH conditions, which facilitated the permeation of organelle membrane. Furthermore, in the presence of a cytosolic ATP concentration, the nanogels could degrade and release the drug payload in the cytosol. This new approach allows for a well-defined release of encapsulated drugs and showed higher efficacy than the free MTX.

Positively charged nanoparticles possess higher affinity to the negatively charged cell membrane, which facilitates cellular uptake, whereas their severe cytotoxicity, strong interactions with blood components, and rapid clearance impede the in vivo applications. We fabricated a biodegradable zwitterionic nanogel with two-stage charge conversional properties for therapeutic protein delivery. The introduction of citraconic anhydride is, on the one hand, to provide carboxyl groups for complexing cytochrome C and offering the zwitterionic property for the first-stage charge conversion in the tumor extracellular environment, and, on the other hand, to form pH-cleavable citraconic amide that can release amino groups under the acidic organelle conditions for the second-stage charge conversion. Having escaped from the endosome, CC could be efficiently released due to the dissociation of the nanogel in the ATP-containing cytosol, which resulted in cell death by mitochondria dependent apoptosis.

In the future, other pH cleavable linkers like β-thiopropionate, should be applied in the formation of biodegradable nanogels. Moreover, the nanoprecipitation method is facing a tremendous challenge in scaling up the production, which needs to be further improved. In addition, co-encapsulation of hydrophobic and hydrophilic drugs might be achieved in core-shell nanogels. To enhance the specific cellular uptake of neutral or negative nanogel particles those are usually less toxic but possess lower internalization efficiency compared to positive ones, the nanogels can be decorated with targeting moieties, such as antibodies, peptides, or small molecules.

5 Zusammenfassung und Ausblick

In der vorliegenden Arbeit wurde die inverse Nanofällung, welche eine milde, Tensid-freie und energiesparende Methode darstellt, angewendet, um biodegradierbare Nanogele basierend auf dendritischem Polyglycerol (dPG) herzustellen. Eine Serie dPG-basierter Vorläuferpolymere wurde synthetisiert und diente dazu, die korrespondierenden Nanogelpartikel mit einstellbarer Dimension und geringer Polydispersität während der in situ Gelbildung durch inverse Nanofällung herzustellen. Durch ihr biokompatibles Gerüst stellen diese Nanogele vielversprechende Vehikel für den Transport und die Verabreichung von Krebsmedikamenten und Proteinen dar. Hierbei vermittelt das Nanogel die intrazelluläre Aufnahme des Gastmoleküls und dessen Freisetzung als Reaktion auf ein intrazelluläres Signal.

Die Thiol-Disulfid-Austauschreaktion wurde dafür verwendet ein System zu entwickeln, welches sowohl sensitiv auf Unterschiede im pH-Wert als auch im Redox-Potential reagiert und somit verschiedene intrazelluläre Signale ausnützt. Als makromolekulare Vorstufe wurde dPG mit Liponsäure funktionalisiert. Eine geringe Menge Dithiothreitol (DTT) wurde dazu verwendet den Lipoyl-Ring zu spalten und dadurch Dihydrolipoyl-Gruppen zu generieren, welche die Thiol-Disulfid-Austauschreaktion initiieren. Eine Degradierung des durch Disulfidbrücken quervernetzten Netzwerk zu kleinen Fragmenten, welche vom Körper ausgeschieden und beseitigt werden können, wurde unter intrazellulären Redox-Bedingungen erreicht. An diese Nanogele wurde das Krebsmedikament Doxorubicin (DOX) kovalent über einen Säure-labilen Hydrazon-Linker, welcher unter physiologischen Bedingungen stabil ist, jedoch in sauren Zellorganellen gespalten wird, an das Nanogel, konjugiert. Es konnte gezeigt werden, dass dieses Prodrug-Nanogel (pharmokologisch unwirksames Vorläufer-Nanogel) effizient in Zellen aufgenommen wird, das wirksame Medikament als Reaktion auf die intrazelluläre Umgebung abgibt und ultimativ zum Tod von (Krebs-) Zellen führt.

Die zytosolisch erhöhte ATP-Konzentration kann als weiteres prominentes intrazelluläres Signal verwendet werden. Hierzu wurde ein degradierbares Nanogel für den intrazellulären Transport von Krebsmedikamenten entwickelt, welches auf einen niedrigen pH und einen erhöhten ATP-Spiegel reagiert. Die Quervernetzung der Nanogele erfolgt durch Boronat/Borat-Ester-Brücken zwischen den 1,2-Diolen des dPG und Boronsäuren. Das Krebsmedikament Methotrexat (MTX) wurde durch elektrostatische Wechselwirkungen in das Nanogel verkapselt und unter Einwirkung von erhöhter ATP-Komzentration oder saurem pH schnell freigesetzt. die Nanogele schwellen bei saurem pH, wie er in sauren Zellorganellen herrscht, an und fördern dadurch die Permeation durch die Zellorganellenmembran. Darüber hinaus konnte gezeigt werden, dass die Nanogele im Cytosol durch den erhöhten ATP-Gehalt degradieren und ihre Ladung freisetzen. Dieser neue Ansatz erlaubt es, das verkapselte Medikament definiert und zielgenau freizusetzen und dadurch dessen Wirkung gegenüber dem freien MTX zu verstärken.

Positiv geladene Nanopartikel besitzen eine höhere Affinität zu den negativ geladenen Zellmembranen, wodurch ihre zelluläre Aufnahme gefördert wird. Allerdings erhöht sich dadurch auch die Zytotoxizität, es treten stärkere Wechselwirkungen mit Blutbestandteilen auf und die Clearance (Beseitigung aus der Blutbahn) ist beschleunigt, weshalb in vivo Applikationen nicht in Frage kommen. Um diese Probleme zu umgehen, wurde ein degradierbares zwitterionisches Nanogel, welches seine Ladung in zwei Stufen konvertieren kann, für den Transport von therapeutischen Proteinen entwickelt. Durch Einführung von Citraconsäureanhydrid in das Nanogel werden zum einen Carboxygruppen zur Komplexierung von Cytochrom C (CC) bereitgestellt sowie die zwitterionischen Eigenschaften für die erste Stufe der Ladungsumwandlung auf Grund der extrazellulären Bedingungen im Tumorgewebe vermittelt, zum anderen wird das pH-spaltbare Citraconicamid gebildet, welches bei saurem Zellorganell-pH Aminogruppen für die zweite Stufe der Ladungsumwandlung abspalten kann. Nach dem Austritt aus dem Endosom kann das CC effizient freigesetzt werden, da das Nanogel durch den erhöhten ATP-Gehalt im Cytosol dissoziiert. Dies führt zu zum Zelltod durch Mitochondrien-abhängige

Apoptose.

In Zukunft könnten weitere spaltbare Linker wie Didodecyl-3,3'-thiodipropionat zur Bildung von biodegradierbaren Nanogelen verwendet werden. Zudem stellt die Nanofällung in größerem Maßstab eine weitere Herausforderung dar. Darüber hinaus bergen Kern-Schale-Architekturen das Potential hydrophobe und hydrophile Medikamente gleichzeitig zu verkapseln. Die spezifische Aufnahme von neutralen oder negativ geladenen Nanopartikeln, welche üblicherweise weniger toxisch sind allerdings schlechter aufgenommen werden als positiv geladene Nanopartikel, könnte durch Dekoration der Nanogele mit spezifischen Zielmolekülen, z.B. Antikörpern, Peptiden oder kleinen Molekülen, verbessert werden.

6 References

[1] a) K. Raemdonck, J. Demeester, S. De Smedt, *Soft Matter* **2009**, *5*, 707-715; b) H. Wei, R. X. Zhuo, X. Z. Zhang, *Prog. Polym. Sci.* **2013**, *38*, 503-535.

[2] Y. Zhang, H. F. Chan, K. W. Leong, *Adv. Drug Deliver. Rev.* **2013**, *65*, 104-120.

[3] a) J. Gong, M. Chen, Y. Zheng, S. Wang, Y. Wang, *J. Control. Release* **2012**, *159*, 312-323; b) N. Nasongkla, E. Bey, J. Ren, H. Ai, C. Khemtong, J. S. Guthi, S.-F. Chin, A. D. Sherry, D. A. Boothman, J. Gao, *Nano Lett.* **2006**, *6*, 2427-2430; c) K. Miyata, R. J. Christie, K. Kataoka, *React. Funct. Polym.* **2011**, *71*, 227-234.

[4] a) T. M. Allen, P. R. Cullis, *Adv. Drug Deliver. Rev.* **2013**, *65*, 36-48; b) W. T. Al-Jamal, K. Kostarelos, *Acc. Chem. Res.* **2011**, *44*, 1094-1104.

[5] a) W. H. De Jong, P. J. A. Borm, *Eur. J. Nanomed.* **2008**, *3*, 133-149; b) S. Parveen, R. Misra, S. K. Sahoo, *Nanomed.-Nanotechnol. Biol. Med.* **2012**, *8*, 147-166.

[6] a) E. A. Murphy, B. K. Majeti, R. Mukthavaram, L. M. Acevedo, L. A. Barnes, D. A. Cheresh, *Mol. Cancer Ther.* **2011**, *10*, 972-982; b) A. Sharma, T. Garg, A. Aman, K. Panchal, R. Sharma, S. Kumar, T. Markandeywar, *Artif. Cells Blood Substit. Immobil. Biotechnol.* **2014**, 1-13.

[7] a) P. Kesharwani, K. Jain, N. K. Jain, *Prog. Polym. Sci.* **2014**, *39*, 268-307; b) B. K. Nanjwade, H. M. Bechra, G. K. Derkar, F. V. Manvi, V. K. Nanjwade, *Eur. J. Pharm. Sci.* **2009**, *38*, 185-196.

[8] a) W. Chen, K. Achazi, B. Schade, R. Haag, *Journal of Controlled Release*; b) S. Mura, J. Nicolas, P. Couvreur, *Nat. Mater.* **2013**, *12*, 991-1003; c) M. M. Yallapu, M. Jaggi, S. C. Chauhan, *Drug Discov. Today* **2011**, *16*, 457-463; d) Y. Li, G. H. Gao, D. S. Lee, *Adv. Healthc. Mater.* **2013**, *2*, 388-417.

[9] a) K. Cho, X. Wang, S. Nie, Z. Chen, D. M. Shin, *Clin. Cancer Res.* **2008**, *14*, 1310-1316; b) C. S. Kim, B. Duncan, B. Creran, V. M. Rotello, *Nano Today* **2013**, *8*, 439-447.

[10] X. Wei, T. H. Senanayake, G. Warren, S. V. Vinogradov, *Bioconjugate Chem.* **2013**, *24*, 658-668.

[11] X. Shuai, T. Merdan, A. K. Schaper, F. Xi, T. Kissel, *Bioconjugate Chem.* **2004**, *15*, 441-448.

[12] P. Lemieux, S. Vinogradov, C. Gebhart, N. Guerin, G. Paradis, H. K. Nguyen, B. Ochietti, Y. Suzdaltseva, E. Bartakova, T. Bronich, Y. St-Pierre, V. Alakhov, A. Kabanov, *J. Drug Target.* **2000**, *8*, 91-105.

[13] a) M. H. Nelson, D. A. Stein, A. D. Kroeker, S. A. Hatlevig, P. L. Iversen, H. M. Moulton, *Bioconjugate Chem.* **2005**, *16*, 959-966; b) A. Ezra, A. Hoffman, E. Breuer, I. S. Alferiev, J. Mönkkönen, N. El Hanany-Rozen, G. Weiss, D. Stepensky, I. Gati, H. Cohen, S. Törmälehto, G. L. Amidon, G. Golomb, *J. Mater. Chem.* **2000**, *43*, 3641-3652.

[14] a) L. Tao, G. Mantovani, F. Lecolley, D. M. Haddleton, *J. Am. Chem. Soc.*

2004, *126*, 13220-13221; b) S. Zalipsky, N. Mullah, C. Engbers, M. U. Hutchins, R. Kiwan, *Bioconjugate Chem.* **2007**, *18*, 1869-1878.

[15] a) X. Yang, H. Hong, J. J. Grailer, I. J. Rowland, A. Javadi, S. A. Hurley, Y. Xiao, Y. Yang, Y. Zhang, R. J. Nickles, W. Cai, D. A. Steeber, S. Gong, *Biomaterials* **2011**, *32*, 4151-4160; b) F. Zhan, W. Chen, Z. Wang, W. Lu, R. Cheng, C. Deng, F. Meng, H. Liu, Z. Zhong, *Biomacromolecules* **2011**, *12*, 3612-3620.

[16] a) W. J. Parak, D. Gerion, D. Zanchet, A. S. Woerz, T. Pellegrino, C. Micheel, S. C. Williams, M. Seitz, R. E. Bruehl, Z. Bryant, C. Bustamante, C. R. Bertozzi, A. P. Alivisatos, *Chem. Mater.* **2002**, *14*, 2113-2119; b) M. Oishi, Y. Nagasaki, K. Itaka, N. Nishiyama, K. Kataoka, *J. Am. Chem. Soc.* **2005**, *127*, 1624-1625.

[17] R. Duncan, M. J. Vicent, *Adv. Drug Deliver. Rev.* **2010**, *62*, 272-282.

[18] G. Pasut, F. M. Veronese, *Prog. Polym. Sci.* **2007**, *32*, 933-961.

[19] R. T. Chacko, J. Ventura, J. Zhuang, S. Thayumanavan, *Adv. Drug Deliver. Rev.* **2012**, *64*, 836-851.

[20] F. Danhier, O. Feron, V. Préat, *J. Control. Release* **2010**, *148*, 135-146.

[21] W. C. Chen, A. X. Zhang, S. D. Li, *Eur. J. Nanomed.* **2012**, *4*, 89-93.

[22] R. Haag, F. Kratz, *Angew. Chem. Int. Ed.* **2006**, *45*, 1198-1215.

[23] A. K. Iyer, G. Khaled, J. Fang, H. Maeda, *Drug Discov. Today* **2006**, *11*, 812-818.

[24] a) H. Maeda, G. Y. Bharate, J. Daruwalla, *Eur. J. Pharm. Biopharm.* **2009**, *71*, 409-419; b) H. Maeda, T. Sawa, T. Konno, *J. Control. Release* **2001**, *74*, 47-61; c) R. K. Jain, *Cancer Res.* **1987**, *47*, 3039-3051.

[25] H. Kobayashi, R. Watanabe, P. L. Choyke, *Theranostics* **2014**, *4*, 81-89.

[26] a) X. Zhang, S. Malhotra, M. Molina, R. Haag, *Chem. Soc. Rev.* **2015**, *44*, 1948-1973; b) X. Zhang, K. Achazi, D. Steinhilber, F. Kratz, J. Dernedde, R. Haag, *Journal of Controlled Release* **2014**, *174*, 209-216; c) Y. Sasaki, K. Akiyoshi, *Chem. Rec.* **2010**, *10*, 366-376.

[27] J. K. Oh, D. I. Lee, J. M. Park, *Prog. Polym. Sci.* **2009**, *34*, 1261-1282.

[28] A. V. Kabanov, S. V. Vinogradov, *Angew. Chem.Int. Ed.* **2009**, *48*, 5418-5429.

[29] a) N. Sanson, J. Rieger, *Polym. Chem.* **2010**, *1*, 965-977; b) J. Ramos, J. Forcada, R. Hidalgo-Alvarez, *Chem. Rev.* **2013**, *114*, 367-428; c) J. K. Oh, D. J. Siegwart, H.-i. Lee, G. Sherwood, L. Peteanu, J. O. Hollinger, K. Kataoka, K. Matyjaszewski, *J. Am. Chem. Soc.* **2007**, *129*, 5939-5945; d) D. J. Siegwart, A. Srinivasan, S. A. Bencherif, A. Karunanidhi, J. K. Oh, S. Vaidya, R. Jin, J. O. Hollinger, K. Matyjaszewski, *Biomacromolecules* **2009**, *10*, 2300-2309.

[30] a) J. K. Oh, S. A. Bencherif, K. Matyjaszewski, *Polymer* **2009**, *50*, 4407-4423; b) S. E. Averick, A. J. D. Magenau, A. Simakova, B. F. Woodman, A. Seong, R. A. Mehl, K. Matyjaszewski, *Polym. Chem.* **2011**, *2*, 1476-1478.

[31] a) J. A. Prescher, D. H. Dube, C. R. Bertozzi, *Nature* **2004**, *430*, 873-877; b) E. M. Sletten, C. R. Bertozzi, *Acc. Chem. Res.* **2011**, *44*, 666-676; c) J. A. Prescher, C. R. Bertozzi, *Nat Chem Biol* **2005**, *1*, 13-21; d) E. M. Sletten, C. R. Bertozzi, *Angew. Chem. In. Ed.* **2009**, *48*, 6974-6998; e) H. C. Hang, C. Yu, D.

L. Kato, C. R. Bertozzi, *PNAS* **2003**, *100*, 14846-14851.
[32] a) D. Steinhilber, M. Witting, X. Zhang, M. Staegemann, F. Paulus, W. Friess, S. Küchler, R. Haag, *J. Control. Release* **2013**, *169*, 289-295; b) D. A. Heller, Y. Levi, J. M. Pelet, J. C. Doloff, J. Wallas, G. W. Pratt, S. Jiang, G. Sahay, A. Schroeder, J. E. Schroeder, Y. Chyan, C. Zurenko, W. Querbes, M. Manzano, D. S. Kohane, R. Langer, D. G. Anderson, *Adv. Mater.* **2013**, *25*, 1449-1454.
[33] M. G. Finn, V. V. Fokin, *Chem. Soc. Rev.* **2010**, *39*, 1231-1232.
[34] J. C. Jewett, C. R. Bertozzi, *Chem. Soc. Rev.* **2010**, *39*, 1272-1279.
[35] Y. Jiang, J. Chen, C. Deng, E. J. Suuronen, Z. Zhong, *Biomaterials* **2014**, *35*, 4969-4985.
[36] V. X. Truong, M. P. Ablett, H. T. J. Gilbert, J. Bowen, S. M. Richardson, J. A. Hoyland, A. P. Dove, *Biomater. Sci.* **2014**, *2*, 167-175.
[37] D. Steinhilber, T. Rossow, S. Wedepohl, F. Paulus, S. Seiffert, R. Haag, *Angew. Chem. Int. Ed.* **2013**, *52*, 13538-13543.
[38] E. Hachet, N. Sereni, I. Pignot-Paintrand, V. Ravaine, A. Szarpak-Jankowska, R. Auzély-Velty, *J. Colloid Interf. Sci.* **2014**, *419*, 52-55.
[39] B. D. Mather, K. Viswanathan, K. M. Miller, T. E. Long, *Prog. Polym. Sci.* **2006**, *31*, 487-531.
[40] T. Rossow, J. A. Heyman, A. J. Ehrlicher, A. Langhoff, D. A. Weitz, R. Haag, S. Seiffert, *J. Am. Chem. Soc.* **2012**, *134*, 4983-4989.
[41] A. K. Engel, T. Yoden, K. Sanui, N. Ogata, *J. Am. Chem. Soc.* **1985**, *107*, 8308-8310.
[42] Y. Xin, J. Yuan, *Polym. Chem.* **2012**, *3*, 3045-3055.
[43] P. R. Sarika, P. R. Anil Kumar, D. K. Raj, N. R. James, *Carbohyd. Polym.* **2015**, *119*, 118-125.
[44] P. A. Fernandes, M. J. Ramos, *Chem. Eur. J.* **2004**, *10*, 257-266.
[45] C. S. Sevier, C. A. Kaiser, *Nat. Rev. Mol. Cell Biol.* **2002**, *3*, 836-847.
[46] a) R. Bahadur K. C, P. Xu, *Adv. Mater.* **2012**, *24*, 6479-6483; b) J.-H. Ryu, S. Bickerton, J. Zhuang, S. Thayumanavan, *Biomacromolecules* **2012**, *13*, 1515-1522.
[47] a) L. Li, K. Raghupathi, C. Yuan, S. Thayumanavan, *Chem. Sci.* **2013**, *4*, 3654-3660; b) D. C. González-Toro, J.-H. Ryu, R. T. Chacko, J. Zhuang, S. Thayumanavan, *J. Am. Chem. Soc.* **2012**, *134*, 6964-6967; c) J. H. Ryu, S. Jiwpanich, R. Chacko, S. Bickerton, S. Thayumanavan, *J. Am. Chem. Soc.* **2010**, *132*, 8246-8247.
[48] a) J. He, B. Yan, L. Tremblay, Y. Zhao, *Langmuir* **2010**, *27*, 436-444; b) J. He, X. Tong, Y. Zhao, *Macromolecules* **2009**, *42*, 4845-4852; c) Y. C. Wang, J. Wu, Y. Li, J. Z. Du, Y. Y. Yuan, J. Wang, *Chem. Commun.* **2010**, *46*, 3520-3522.
[49] C. G. Williams, A. N. Malik, T. K. Kim, P. N. Manson, J. H. Elisseeff, *Biomaterials* **2005**, *26*, 1211-1218.
[50] a) J. Zhuang, S. Jiwpanich, V. D. Deepak, S. Thayumanavan, *ACS Macro Lett.* **2011**, *1*, 175-179; b) M. A. Pujana, L. Pérez-Álvarez, L. C. Cesteros Iturbe, I. Katime, *Polymer* **2012**, *53*, 3107-3116.
[51] C. W. Park, H. M. Yang, H. J. Lee, J. D. Kim, *Soft Matter* **2013**, *9*, 1781-1788.

[52] a) M. Piest, X. Zhang, J. Trinidad, J. F. J. Engbersen, *Soft Matter* **2011**, *7*, 11111-11118; b) A. Mahalingam, J. I. Jay, K. Langheinrich, S. Shukair, M. D. McRaven, L. C. Rohan, B. C. Herold, T. J. Hope, P. F. Kiser, *Biomaterials* **2011**, *32*, 8343-8355; c) J. I. Jay, S. Shukair, K. Langheinrich, M. C. Hanson, G. C. Cianci, T. J. Johnson, M. R. Clark, T. J. Hope, P. F. Kiser, *Adv. Funct. Mater.* **2009**, *19*, 2969-2977; d) M. C. Roberts, M. C. Hanson, A. P. Massey, E. A. Karren, P. F. Kiser, *Adv. Mater.* **2007**, *19*, 2503-2507; e) L. He, D. E. Fullenkamp, J. G. Rivera, P. B. Messersmith, *Chem. Commun.* **2011**, *47*, 7497-7499; f) J. Xu, D. Yang, W. Li, Y. Gao, H. Chen, H. Li, *Polymer* **2011**, *52*, 4268-4276.

[53] a) W. Chen, Y. Cheng, B. Wang, *Angew. Chem. Int. Ed.* **2012**, *51*, 5293-5295; b) Y. Li, W. Xiao, K. Xiao, L. Berti, J. Luo, H. P. Tseng, G. Fung, K. S. Lam, *Angew. Chem. Int. Ed.* **2012**, *51*, 2864-2869.

[54] a) T. Aikawa, T. Konno, M. Takai, K. Ishihara, *Langmuir* **2011**, *28*, 2145-2150; b) Y. Kotsuchibashi, R. V. C. Agustin, J. Y. Lu, D. G. Hall, R. Narain, *ACS Macro Lett.* **2013**, *2*, 260-264; c) X. Zhang, K. Achazi, R. Haag, *Adv. Healthc. Mater.* **2015**, *4*, 585-592.

[55] a) D. J. Menzies, A. Cameron, T. Munro, E. Wolvetang, L. Grøndahl, J. J. Cooper-White, *Biomacromolecules* **2012**, *14*, 413-423; b) K. M. Park, Y. Lee, J. Y. Son, D. H. Oh, J. S. Lee, K. D. Park, *Biomacromolecules* **2012**, *13*, 604-611.

[56] C. Wu, C. Bottcher, R. Haag, *Soft Matter* **2015**, *11*, 972-980.

[57] a) K. Kim, B. Bae, Y. J. Kang, J.-M. Nam, S. Kang, J.-H. Ryu, *Biomacromolecules* **2013**, *14*, 3515-3522; b) T. Nakai, T. Hirakura, Y. Sakurai, T. Shimoboji, M. Ishigai, K. Akiyoshi, *Macromol. Biosci.* **2012**, *12*, 475-483.

[58] a) Y. W. Noh, S. H. Kong, D. Y. Choi, H. S. Park, H. K. Yang, H. J. Lee, H. C. Kim, K. W. Kang, M. H. Sung, Y. T. Lim, *ACS Nano* **2012**, *6*, 7820-7831; b) U. Hasegawa, S. M. Nomura, S. C. Kaul, T. Hirano, K. Akiyoshi, *Biochem. Bioph. Res. Co.* **2005**, *331*, 917-921; c) M. Fujioka-Kobayashi, M. S. Ota, A. Shimoda, K. Nakahama, K. Akiyoshi, Y. Miyamoto, S. Iseki, *Biomaterials* **2012**, *33*, 7613-7620; d) U. Hasegawa, S. Sawada, T. Shimizu, T. Kishida, E. Otsuji, O. Mazda, K. Akiyoshi, *J. Control. Release* **2009**, *140*, 312-317; e) T. Hirakura, K. Yasugi, T. Nemoto, M. Sato, T. Shimoboji, Y. Aso, N. Morimoto, K. Akiyoshi, *J. Control. Release* **2010**, *142*, 483-489; f) Y. Sekine, Y. Moritani, T. Ikeda-Fukazawa, Y. Sasaki, K. Akiyoshi, *Adv. Healthc. Mater.* **2012**, *1*, 722-728.

[59] K. H. Bae, H. Mok, T. G. Park, *Biomaterials* **2008**, *29*, 3376-3383.

[60] S. Singh, F. Topuz, K. Hahn, K. Albrecht, J. Groll, *Angew. Chem. Int. Ed.* **2013**, *52*, 3000-3003.

[61] C. Fasting, C. A. Schalley, M. Weber, O. Seitz, S. Hecht, B. Koksch, J. Dernedde, C. Graf, E. W. Knapp, R. Haag, *Angew. Chem. Int. Ed.* **2012**, *51*, 10472-10498.

[62] a) G. Pan, Q. Guo, C. Cao, H. Yang, B. Li, *Soft Matter* **2013**, *9*, 3840-3850; b) X. Lu, M. Sun, A. E. Barron, *J. Colloid Interf. Sci.* **2011**, *357*, 345-353; c) L.

W. Xia, R. Xie, X. J. Ju, W. Wang, Q. Chen, L. Y. Chu, *Nat. Commun.* **2013**, *4*.
[63] a) G. R. Hendrickson, M. H. Smith, A. B. South, L. A. Lyon, *Adv. Funct. Mater.* **2010**, *20*, 1697-1712; b) J. K. Oh, R. Drumright, D. J. Siegwart, K. Matyjaszewski, *Prog. Polym. Sci.* **2008**, *33*, 448-477.
[64] a) S. Seiffert, *ChemPhysChem* **2013**, *14*, 295-304; b) I. A. Eydelnant, B. Betty Li, A. R. Wheeler, *Nat Commun* **2014**, *5*; c) Y. Du, E. Lo, S. Ali, A. Khademhosseini, *PNAS* **2008**, *105*, 9522-9527.
[65] a) E. M. Enlow, J. C. Luft, M. E. Napier, J. M. DeSimone, *Nano Lett.* **2011**, *11*, 808-813; b) T. J. Merkel, S. W. Jones, K. P. Herlihy, F. R. Kersey, A. R. Shields, M. Napier, J. C. Luft, H. Wu, W. C. Zamboni, A. Z. Wang, J. E. Bear, J. M. DeSimone, *PNAS* **2011**, *108*, 586-591.
[66] J. P. Rolland, B. W. Maynor, L. E. Euliss, A. E. Exner, G. M. Denison, J. M. DeSimone, *J. Am. Chem. Soc.* **2005**, *127*, 10096-10100.
[67] Y. Wang, J. D. Byrne, M. E. Napier, J. M. DeSimone, *Adv. Drug Deliver. Rev.* **2012**, *64*, 1021-1030.
[68] M. E. Napier, J. M. DeSimone, *Polym. Rev.* **2007**, *47*, 321-327.
[69] A. V. Kabanov, S. V. Vinogradov, *Angew. Chem. Int. Ed.* **2009**, *48*, 5418-5429.
[70] a) T. Govender, S. Stolnik, M. C. Garnett, L. Illum, S. S. Davis, *J. Control. Release* **1999**, *57*, 171-185; b) T. Betancourt, B. Brown, L. Brannon-Peppas, *Nanomedicine* **2007**, *2*, 219-232.
[71] a) J. Lee, S. Hwang, D. Lee, S. Kim, D. Kim, *Macromol. Res.* **2009**, *17*, 72-78; b) Y. Zhang, R. X. Zhuo, *Biomaterials* **2005**, *26*, 6736-6742.
[72] H. Fessi, F. Puisieux, J. P. Devissaguet, N. Ammoury, S. Benita, *Int. J. Pharm.* **1989**, *55*, R1-R4.
[73] E. Fleige, M. A. Quadir, R. Haag, *Adv. Drug Deliver. Rev.* **2012**, *64*, 866-884.
[74] M. Richter, D. Steinhilber, R. Haag, R. von Klitzing, *Macromol. Rapid Comm.* **2014**, *35*, 2018-2022.
[75] a) L. Shi, S. Khondee, T. H. Linz, C. Berkland, *Macromolecules* **2008**, *41*, 6546-6554; b) R. Sunasee, P. Wattanaarsakit, M. Ahmed, F. B. Lollmahomed, R. Narain, *Bioconjugate Chem.* **2012**, *23*, 1925-1933.
[76] a) S. A. Bencherif, N. R. Washburn, K. Matyjaszewski, *Biomacromolecules* **2009**, *10*, 2499-2507; b) K. Raemdonck, B. Naeye, K. Buyens, R. E. Vandenbroucke, A. Høgset, J. Demeester, S. C. De Smedt, *Adv. Funct. Mater.* **2009**, *19*, 1406-1415.
[77] H. Tan, H. Jin, H. Mei, L. Zhu, W. Wei, Q. Wang, F. Liang, C. Zhang, J. Li, X. Qu, D. Shangguan, Y. Huang, Z. Yang, *Soft Matter* **2012**, *8*, 2644-2650.
[78] C. Lu, B. Li, N. Liu, G. Wu, H. Gao, J. Ma, *RSC Adv.* **2014**, *4*, 50301-50311.
[79] N. Morimoto, S. Hirano, H. Takahashi, S. Loethen, D. H. Thompson, K. Akiyoshi, *Biomacromolecules* **2012**, *14*, 56-63.
[80] N. Murthy, Y. X. Thng, S. Schuck, M. C. Xu, J. M. J. Fréchet, *J. Am. Chem. Soc.* **2002**, *124*, 12398-12399.
[81] L. Zhao, L. Zhu, Q. Wang, J. Li, C. Zhang, J. Liu, X. Qu, G. He, Y. Lu, Z. Yang, *Soft Matter* **2011**, *7*, 6144-6150.
[82] Y. Bae, K. Kataoka, *Adv. Drug Deliver. Rev.* **2009**, *61*, 768-784.

[83] W. Chen, M. Zheng, F. Meng, R. Cheng, C. Deng, J. Feijen, Z. Zhong, *Biomacromolecules* **2013**, *14*, 1214-1222.

[84] a) J. Jordan, M. d'Arcy Doherty, G. M. Cohen, *Brit. J. Cancer* **1987**, *55*, 627-631; b) F. Q. Schafer, G. R. Buettner, *Free Radical Bio. Med.* **2001**, *30*, 1191-1212; c) R. Franco, J. A. Cidlowski, *Cell Death Differ* **2009**, *16*, 1303-1314; d) J. M. Estrela, A. Ortega, E. Obrador, *Crit. Rev. Clin. Lab. Sci.* **2006**, *43*, 143-181.

[85] a) A. Russo, W. DeGraff, N. Friedman, J. B. Mitchell, *Cancer Res.* **1986**, *46*, 2845-2848; b) A. Gupte, R. J. Mumper, *Cancer Treat. Rev.* **2009**, *35*, 32-46.

[86] Z.-Y. Qiao, R. Zhang, F.-S. Du, D.-H. Liang, Z.-C. Li, *J. Control. Release* **2011**, *152*, 57-66.

[87] a) M. H. Xiong, Y. J. Li, Y. Bao, X. Z. Yang, B. Hu, J. Wang, *Adv. Mater.* **2012**, *24*, 6175-6180; b) P. M. Kharkar, K. L. Kiick, A. M. Kloxin, *Chem. Soc. Rev.* **2013**, *42*, 7335-7372.

[88] a) C. N. Bowman, C. J. Kloxin, *AIChE J.* **2008**, *54*, 2775-2795; b) C. A. DeForest, K. S. Anseth, *Nat. Chem.* **2011**, *3*, 925-931.

[89] B. D. Fairbanks, S. P. Singh, C. N. Bowman, K. S. Anseth, *Macromolecules* **2011**, *44*, 2444-2450.

[90] N. E. Fedorovich, M. H. Oudshoorn, D. van Geemen, W. E. Hennink, J. Alblas, W. J. A. Dhert, *Biomaterials* **2009**, *30*, 344-353.

[91] a) D. Klinger, K. Landfester, *Macromolecules* **2011**, *44*, 9758-9772; b) M. A. Azagarsamy, D. L. Alge, S. J. Radhakrishnan, M. W. Tibbitt, K. S. Anseth, *Biomacromolecules* **2012**, *13*, 2219-2224; c) I. Tomatsu, K. Peng, A. Kros, *Adv. Drug Deliver. Rev.* **2011**, *63*, 1257-1266.

[92] a) H. L. Wei, Z. Yang, L. M. Zheng, Y. M. Shen, *Polymer* **2009**, *50*, 2836-2840; b) C. M. Nimmo, S. C. Owen, M. S. Shoichet, *Biomacromolecules* **2011**, *12*, 824-830; c) S. Kirchhof, F. P. Brandl, N. Hammer, A. M. Goepferich, *J. Mater. Chem. B* **2013**, *1*, 4855-4864.

[93] a) A. D. Baldwin, K. L. Kiick, *Bioconjugate Chem.* **2011**, *22*, 1946-1953; b) A. D. Baldwin, K. L. Kiick, *Polym. Chem.* **2013**, *4*, 133-143.

[94] M. Marref, N. Mignard, C. Jegat, M. Taha, M. Belbachir, R. Meghabar, *Polym. Int.* **2013**, *62*, 87-98.

[95] M. McNutt, *Science* **2014**, *344*, 1460.

[96] H. J. Zhang, Y. Xin, Q. Yan, L. L. Zhou, L. Peng, J. Y. Yuan, *Macromol. Rapid Comm.* **2012**, *33*, 1952-1957.

[97] a) Y. Nomura, Y. Sasaki, M. Takagi, T. Narita, Y. Aoyama, K. Akiyoshi, *Biomacromolecules* **2004**, *6*, 447-452; b) S. Sawada, Y. Sasaki, Y. Nomura, K. Akiyoshi, *Colloid Polym. Sci.* **2011**, *289*, 685-691.

7 Appendix

7.1 Publications and Conference Contributions

Publications

1. **X. Zhang***, K. Zhang, R. Haag, Multistage, charge conversional, stimuli-responsive nanogels for therapeutic protein delivery. *Biomater. Sci.* **2015**, accepted.

2. **X. Zhang**, S. Malhotra, M. Molina, R. Haag*, Micro- and nanogels with labile crosslinks–from synthesis to biomedical applications. *Chem. Soc. Rev.* **2015**, *44*, 1948-1973.

3. **X. Zhang***, K. Achazi, R. Haag*, Boronate cross-linked ATP- and pH-responsive nanogels for intracellular delivery of anticancer drugs. *Adv. Healthc. Mater.* **2015**, *4*, 585-592.

4. **X. Zhang**, K. Achazi, D. Steinhilber, F. Kratz, J. Dernedde, R. Haag*, A facile approach for dual-responsive prodrug nanogels based on dendritic polyglycerols with minimal leaching. *J. Control. Release* **2014**, *174*, 209-216.

5. D. Steinhilber, M. Witting, **X. Zhang**, M. Staegemann, F. Paulus, W. Friess, S. Küchler, R. Haag*, Surfactant free preparation of biodegradable dendritic polyglycerol nanogels by inverse nanoprecipitation for encapsulation and release of pharmaceutical biomacromolecules. *J. Control. Release* **2013**, *169*, 289-295.

6. S. González-Rodríguez, M.A. Quadir, S. Gupta, **X. Zhang**, V. Spahn, D. Labuz, M. Schmelz, H. Machelska, R. Haag, C. Stein*. Polyglycerol-opioid conjugates - a novel generation of pain killers designed to preclude central side effects. *Nat. Comm.* **2015**, submitted.

7. **X. Zhang**, X.G. Zhang*, Z. Wu, X. Gao, C. Cheng, C. Li*, Z. Wang, A hydrotropic β-cyclodextrin grafted hyperbranched polyglycerol co-polymer for hydrophobic drug delivery. *Acta Biomater.* **2011**, *7*, 585-592.

8. **X. Zhang**, X.G. Zhang*, Z. Wu, X. Gao, S. Shu, Z. Wang, C. Li*,β-Cyclodextrin grafting hyperbranched polyglycerols as carriers for nasal insulin delivery. *Carbohyd. Polymers* **2011**, *84*, 1419-1425.

9. **X. Zhang**, X.G. Zhang*, P. Yu, Y. Han, Y. Li, C. Li*, Hydrotropic polymeric mixed micelles based on functional hyperbranched polyglycerol copolymers as hepatoma-targeting drug delivery system. *J. Pharm. Sci.* **2013**, *102*, 145-153.

10. X. Gao, X.G Zhang*, Z. Wu, **X. Zhang**, Z. Wang, C. Li*, Synthesis and physicochemical characterization of a novel amphiphilic polylactic acid-hyperbranched polyglycerol conjugate for protein delivery. *J. Control. Release* **2009**, *140*, 141-147.

11. X. Gao, X.G. Zhang*, **X. Zhang**, Y. Wang, L. Sun, C. Li*, Amphiphilic polylactic acid-hyperbranched polyglycerol nanoparticles as a controlled release system for poorly water-soluble drugs: physicochemical characterization. *J. Pharm. Pharmaco.* **2011**, *63*, 757-764.

12. X. Gao, X.G. Zhang*, **X. Zhang**, C. Cheng, Z. Wang, C. Li, Encapsulation of BSA in polylactic acid–hyperbranched polyglycerol conjugate nanoparticles: preparation, characterization, and release kinetics. *Polym. Bull.* **2010**, *65*, 787-805.

13. S. Shu, X. Wang, X.G. Zhang*, **X. Zhang**, Z. Wang, C. Li*, Disulfide cross-linked biodegradable polyelectrolyte nanoparticles for the oral delivery of protein drugs. *New J. Chem.* **2009**, *33*, 1882-1887.

14. X. Jin, X.G. Zhang*, Z. Wu, D. Teng, **X. Zhang**, Y. Wang, Z. Wang, C. Li*, Amphiphilic Random Glycopolymer based on phenylboronic acid: synthesis, characterization, and potential as glucose-sensitive matrix. *Biomacromolecules* **2009**, *10*, 1337-1345.

Oral Presentations

X. Zhang, X.G. Zhang

A hydrotropic β-cyclodextrin grafted hyperbranched polyglycerol co-polymer for hydrophobic drug delivery

National biological materials conference, Apri 15th-18th 2010 Chengdu, China.

Poster Presentations

1. **X. Zhang**, R. Haag

   A facile approach towards dual-responsive prodrug nanogels based on dendritic polyglycerol for the restriction of drug leaching under physiological conditions

   4th International Symposium on Biomedical Applications of Dendrimers, Jun, 18th-20th 2014 Lugano, Switzerland.

2. **X. Zhang**, R. Haag

   Boronate crosslinked ATP- and pH-responsive nanogels for intracellular delivery of anticancer drug

   8th international dendritic symposium Jun 23th-27th 2013 Madrid, Spain.

7.2 Curriculum Vitae

For reasons of data protection,

the curriculum vitae is not included in the online version